Master Thesis in Physical Oceanography

Mechanisms affecting the transport of early stages of Norwegian Coastal Cod - a fjord study

Mari Skuggedal Myksvoll

May 30, 2008

UNIVERSITY OF BERGEN
GEOPHYSICAL INSTITUTE

Front picture from Rørstad in Folda by Per Reffhaug, with permission.

Abstract

The fjord system of Sørfolda and Nordfolda situated in northern Norway is used in a model study. Particularly to explore the mechanisms causing separation and mixing of eggs from Arcto-Norwegian Cod (ANC) and Norwegian Coastal Cod (CC).

The Regional Ocean Modeling System (ROMS) simulates the circulation in the fjord, characterized by the estuarine circulation. The major forcing to the fjord system is the fresh water discharge, with its seasonal and interannual variations.

Two extreme years with respect to runoff were chosen to study; 1960 representing a cold and dry year, and 1989 representing a warm and wet year. The estuarine circulation was established during both years, with 1989 generally having a fresher surface layer. The onset of melting season was approximately one month earlier in 1989 compared to 1960.

A particle tracking model was used to transport CC eggs in the fjord system. Particles drifting at fixed depths showed especially larger spread at 1 m depth during 1989 than 1960. Most particles lower in the water column stayed within the fjord system.

The particles was added a dynamical vertical distribution, as a function of buoyancy and mixing. A fresher surface layer in April 1989 compared to 1960 caused a larger fraction of the eggs to be heavier than the brackish layer. When the eggs are situated lower in the water column, the possibility of being transported away is much smaller and the degree of retention is larger. Considering the last part of the spawning period a stronger separation between ANC and CC is observed in 1989 compared to 1960. The results indicate that CC have adapted the buoyancy of eggs to increase retention of eggs inside the fjord system.

From the results it is concluded that CC are self-recruiting and the separation between ANC and CC eggs are strong. Future climate change might enhance the separation between the two populations.

Preface

Only five years ago I had never heard about oceanography, and here I am just finishing my master thesis in physical oceanography! I was planning to study physics, but during my first year at the University I heard about something called oceanography. I became curios and figured out that it had something to do about using physics in the ocean. I have always been fascinated by the ocean and wanted to study physics, so oceanography was perfect for me. So now I have been learning about the big ocean for almost four years, and still just want to learn more. In this country the ocean has been a major resource during generations and will be equally important in the future. The fact that the ocean is changing due to global warming is a major challenge and might cause severe consequences for coastal areas.

I would like to thank my supervisors Svein Sundby and Bjørn Ådlandsvik for giving me the opportunity to write a master thesis at the Institute of Marine Research. They have been most helpful with all kinds of problems and encouraging me all the way. A special thanks to Frode Vikebø for lots of technical support and positive feedback at times of frustration. Thanks to Lars Asplin for inputs on fjord processes and to everyone else in the Oceanography and Climate group at IMR for your always interesting coffee breaks. Also thanks to the people at Geofysen for an encouraging study environment.

Finally, a big thanks to my husband Arve for your patience through all these years of reading and writing and always believing in me. I could never have done this without you!

Bergen May 30, 2008

Mari S. Myksvoll

Contents

Chapter 1

Introduction

Vestfjorden is an ocean bay situated between the Lofoten archipelago and the mainland in northern Norway. This is one of the main spawning sites for the Arcto-Norwegian Cod (*Gadus morhua* L.) (Sundby & Bratland, 1987). The region has been subjected to extensive research activity since the 1860s due to the unique location regarding both cod fisheries and reproduction (Sundby, 1980). The great cod fisheries in Norway have experienced large variations in landings, which initiated the study of physical-biological interactions on cod recruitment. Hjort (1914) hypothesized that the large fluctuations in fish recruitment was due to natural variations in the system and that the year-class strength was determined at an early life stage.

Already in the early 1900s fishermen recognized and described different shapes and colors on cod caught close to the coast and cod caught away from the coast (Rinde *et al.*, 1998). Rollefsen (1933) used otholits to determine the age of cod, and later this was used to define the difference between the two populations, which are now known as the Arcto-Norwegian Cod (ANC) and the Norwegian Coastal Cod (CC). The ANC and CC are considered as separate populations regarding to management and quotas. Early stages of ANC are known to drift over long distances (600-1200 km) (Bergstad *et al.*, 1987) into the Barents Sea for feeding and nursery grounds. They migrate back to the Lofoten area to spawn. This is in large contrast to the CC which spawn at the coast and partly into the fjords (Jakobsen, 1987), and are not known to leave the coastal areas. There are several different populations of CC situated along the Norwegian coast, some might even say every fjord has its own population. Studies from the Norwegian Skagerrak coast show local CC populations with a geographical extent of about 30 km and local retention of early life stages (Knutsen *et al.*, 2007; Jorde *et al.*, 2007; Espeland *et al.*, 2007).

Genetic studies are not fully agreeing on the actual genetic difference be-

tween the two species. Some studies are implying greater differences between individuals in a population than differences between populations (Árnason & Pálsson, 1996; Mork & Giæver, 1999). Others find a marked genetic difference between coastal and Arctic populations suggesting more independent populations than earlier studies (Pogson & Fevolden, 2003)

The first attempt to model transport of cod larvae from Lofoten was done by Ådlandsvik and Sundby (1994). They concluded that a need for higher model resolution was necessary to capture the major variations in the system. Vikebø *et al.* (2005) discussed a physical-biological coupling maintaining the separation of ANC and CC, elaborating on the hypothesis by Sundby (1994), who proposed that the separation could be caused by difference in egg buoyancy between the two populations. A difference in buoyancy between ANC and CC eggs is observed in this area, with the ANC eggs more buoyant (Kjesbu *et al.*, 1992). The pelagic ANC eggs, spawned in the saline coastal waters, are concentrated close to the surface and decreasing with depth, and hence very sensitive to variations in wind-induced mixing (Sundby, 1983). The mesopelagic CC eggs, spawned in the fjords with low-saline surface water, are concentrated lower in the water column, being more dependent on the stratification and hydrography (Sundby, 1991). However, Stenevik *et al.* (2005) showed that the specific gravity of CC eggs at different locations along the Norwegian coast did not vary much, but that the local salinity structure of the water masses determined whether the eggs were pelagically or mesopelagically distributed.

Objectives

The object of this thesis is to investigate how differences in salinity profiles and variations in specific gravity of eggs influence horizontal transport, and contribute to separation and mixing between ANC and CC eggs. Particularly explore whether climate change will affect the extent of separation between the two cod populations. A regional ocean model is used to simulate the circulation in a fjord system during two different years. The first year, 1960, representing a cold and dry year, and the second year, 1989, representing a warm and wet year. Drift patterns of eggs will be modeled with a dynamic vertical distribution using a particle tracking model. The spreading and mixing of eggs will be discussed in relation to the different years.

Content

Chapter 2 contains information about the physical and biological environment of Sørfolda and Nordfolda. In chapter 3 background theory is presented. Chapter 4 includes information regarding methods, the circulation model and the particle tracking model. The results from the circulation model are shown in chapter 5, and the output from the particle tracking model is shown in chapter 6. The discussion is found in chapter 7, summary and conclusions in chapter 8. Appendix A contains data from Folda.

Chapter 2

The physical and biological environment of Sørfolda and Nordfolda

2.1 Location

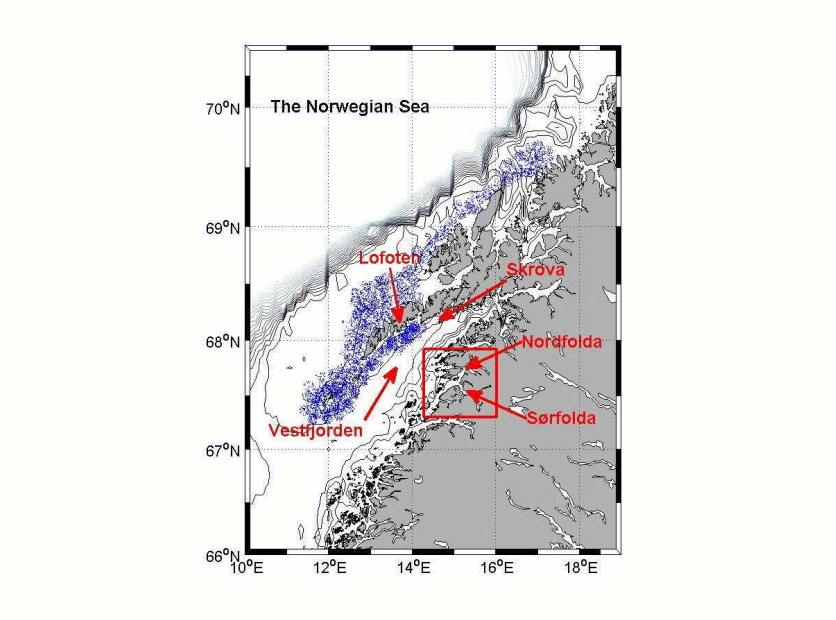

Figure 2.1: Lofoten and Vestfjorden in the northern part of Norway, with the area of study inside the square. The blue shaded area is the main spawning area for ANC.

The fjord system of Nordfolda and Sørfolda is chosen in order to study the separation between Arcto-Norwegian Cod (ANC) and Norwegian Coastal Cod (CC) eggs. These are two separate fjords with a joint opening towards Vestfjorden, located in the northern part of Norway at 67.5°N (see Figure 2.2). The ANC spawn in Vestfjorden and on the northern side of Lofoten, see Figure 2.1, while the CC are known to spawn inside the fjord system of Nordfolda and Sørfolda.

A fjord is often divided into several regions. The innermost part is called the head of the fjord, where the major rivers are located. In a fjord with many branches there are several heads of the fjord system, as shown in Figure 2.2. The place where the fjord widens and meet the coastal areas outside is called the mouth of the fjord.

Nordfolda is 55.6 km long, from mouth to head, and the width is ranging from 4 km to 2.4 km in the innermost part. The greatest depth in Nordfolda is 527 m close to the head, with a sill depth of 225 m. Sørfolda is 50 km long and 3 km wide near the mouth and getting narrower towards the head, reaching a width of 1.6 km at the innermost part. The deepest basin is 574 m deep, and a sill 265 m deep is situated close to the connecting point with Nordfolda (Aure & Pettersen, 2004). The inner end of Sørfolda is divided into two main branches, where the northern part is called Leirfjorden. The whole fjord system is divided into several smaller branches and surrounded by steep mountains.

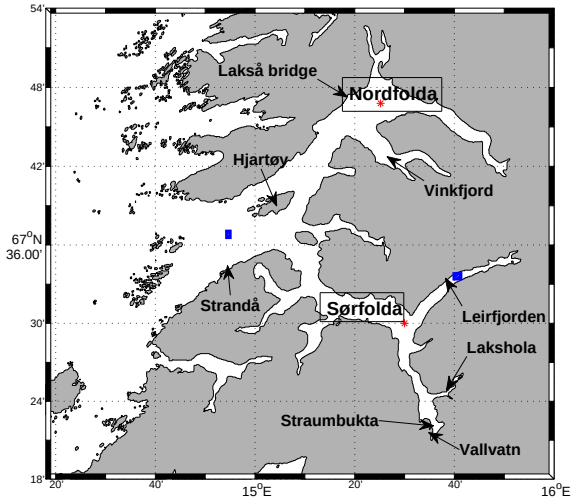

Figure 2.2: The fjord system of Nordfolda and Sørfolda.

2.2 Fresh water input

There are several large rivers discharging great amounts of water into the fjord system. Due to the location at a high latitude the amplitude of the seasonal cycle is large (Sundby, 1982). In winter large amounts of fresh water is retained as snow in the mountains. Melting season starts in late spring and the volume flux is maximized in June (see Figure 4.3). In coastal areas and at lower altitudes (<100 m) the seasonal cycle is different with several floods during the year. The fjord system of Sørfolda and Nordfolda is so large that it covers both coastal and mountain areas. Most of the land area surrounding Nordfolda has middle altitude (100-600 m) and is then considered to be a transition area, between coastal and mountain. The inner part of Sørfolda and Leirfjorden is surrounded by mountains and glaciers, the rest by lower mountains. The rivers discharging at the head of Sørfolda and Leirfjorden have large drainage areas, causing large volume fluxes during the melting season. These two places are the dominating fresh water sources to the system. The fresh water input to Nordfolda is much smaller compared to Sørfolda, and with a different seasonal cycle. This might set up differences between the fjords regarding to salinity and volume fluxes of brackish water.

The spawning is known to occur during spring. This is a transition time regarding the fresh water cycle, going from retention to melting. Differing onset of melting season causing changes in the estuarine circulation, might have a large impact on the transport of eggs. Interannual variability in temperature and precipitation can cause large variations in runoff. In cold years the melting is delayed, whereas during warm years the melting starts earlier and some runoff might even occur during the winter.

2.3 Hydrography

The Institute of Marine Research has been monitoring several fjords in Norway every year since 1975, included Sørfolda and Nordfolda (Aure & Pettersen, 2004). Data have been collected every fall around November/December (Figure 2.3), a season with low primary production and reduced variability in the fjord basins. The salinity profiles (at the right in Figure 2.3(a) and 2.3(b)) show a low-saline surface layer with large interannual variability. Sørfolda has in general a fresher surface layer than Nordfolda, both have lowest salinity at the head. The temperature profiles (at the left in Figure 2.3(a) and 2.3(b)) show large variability in the upper 150 m. The temperature maximum is found around 50-75 m and the highest temperatures are observed in the outer part of the fjord system.

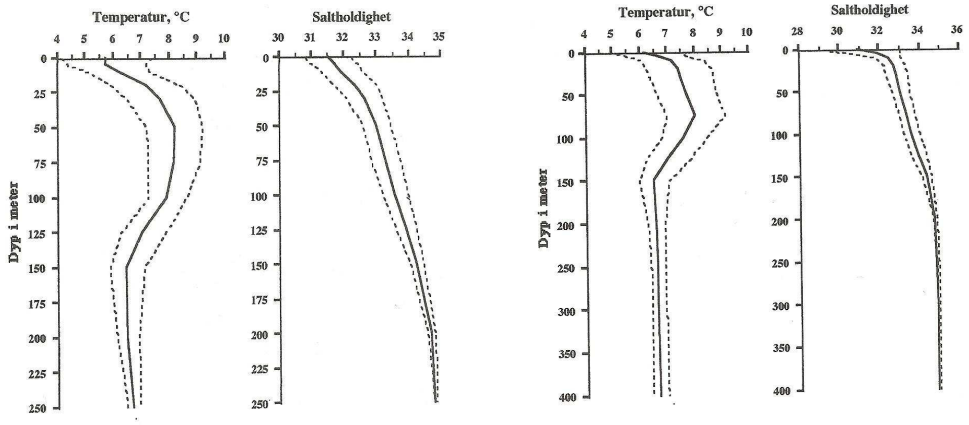

(a) Nordfolda (b) Sørfolda

(Aure & Pettersen, 2004)

Figure 2.3: Mean and standard deviation in temperature and salinity profile from November/December 1976-2001 from the stations at the positions shown in Figure 2.2 as red dots.

2.4 Circulation

The circulation pattern in Sørfolda and Nordfolda is not known in detail. However, all available information suggests the fjord system to be a typical Norwegian fjord with the corresponding estuarine circulation, depending on the fresh water input. The currents in the mouth area are dominated by the tidal cycle (Statens Kartverk, 1998), but vary strongly with changing winds. In both Sørfolda and Nordfolda the prevailing surface currents are directed out of the fjord, but might be influenced by tides when the runoff is reduced and the winds are calm. At the mouth the current is most often directed outwards, especially on the northern side.

Mohus and Haakstad (1984) investigated the physical, chemical and biological conditions in Straumbukta at the inner end of Sørfolda. They sampled hydrographical data seven times from January to November, also currents were measured in November. The circulation pattern was quite complicated but was characterized by the estuarine circulation, with outflow in the upper layer and compensating inflow below. The surface current was also found to vary strongly with the local winds, holding the potential to spin up the estuarine circulation or reverse the whole system. Under normal conditions in Sørfolda the surface current was observed to be 5% of the wind speed.

2.5 Winds

Sundby (1982) investigated the variability and energy of winds in Vestfjorden. The results showed that two different directions are most common in this area, easterly and south-westerly winds. The easterly winds occur specially in winter due to drainage of cold air from the mainland. Cold and heavy airmasses flow out of the fjords and towards the coast following the terrain. Just outside Folda this gives south-easterly winds and north-easterly on the opposite side of Vestfjorden. The south-westerly winds contain more energy but are not as frequent, and occur when low-pressure systems pass by. Under these conditions the winds are directed into Vestfjorden and it is expected that the topography modifies the wind directions further inside Folda.

Inside a fjord with steep sides the wind is assumed to be directed along the fjord. If it is not too wide, there are little variance across the fjord. Channeling of winds in fjords is observed to cause strong winds. The wind direction inside a fjord cannot be predicted from measurements outside. This interaction is complex and also depends on the stability of the atmosphere (Asplin *et al.*, 2002).

2.6 Cod spawning and juvenile distribution

The data available regarding spawning and nursery grounds in Nordfolda and Sørfolda are presented in Figure 2.4. The data have been distributed by The Norwegian Directorate of Fisheries (Gyda Lorås, pers.comm.). Figure 2.4(a) shows that spawning takes place at several locations in the fjord system, particularly at the head of the various fjord arms. Figure 2.4(b) shows the nursery grounds to be mostly situated in Sørfolda except in the inner most end of Nordfolda. This proves Nordfolda and Sørfolda to be well suited for studying the drift of cod eggs.

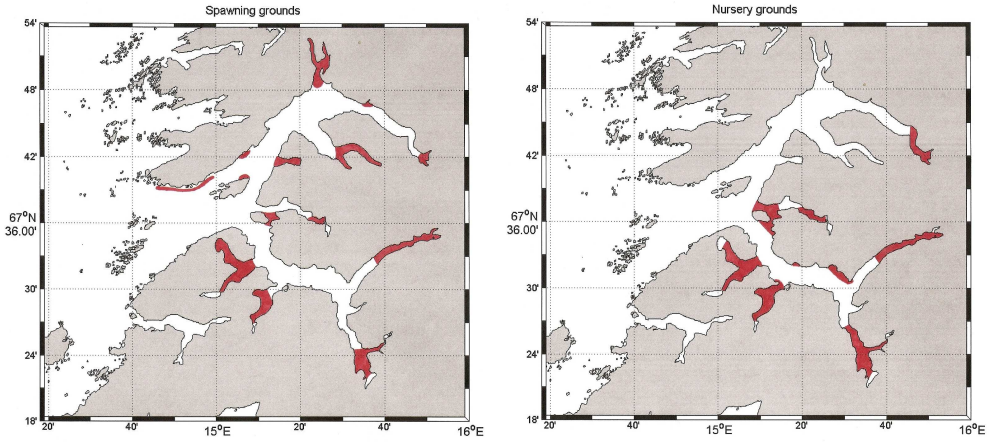

(a) Spawning grounds (b) Nursery grounds

Figure 2.4: Observed spawning and nursery grounds for cod (Gyda Lorås, The Norwegian Directorate of fisheries, pers.comm.).

Chapter 3

Theory

3.1 The estuarine circulation

Fresh water from river runoff meets salty water from the ocean inside the fjord. The physical environment in a fjord system is highly depending on the balance between these two water masses. When the river discharge is

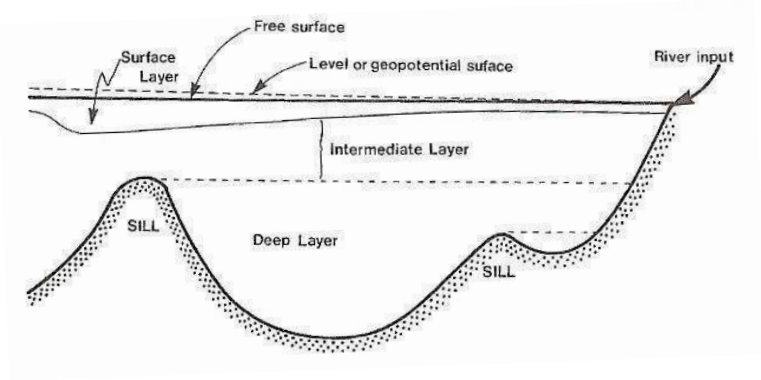

(Farmer & Freeland, 1983)

Figure 3.1: Schematic view of a fjord divided into three layers.

dominating over tidal input the estuarine circulation develops, which is characterized by strong stratification (Dyer, 1997). The fjord can be divided into three layers, a thin surface layer, an intermediate layer and a deep bottom layer below the sill (Figure 3.1). Fjords are often characterized by one or multiple sills, separating the fjord basin from the coastal areas. The deepest part of the fjord can be deeper than the continental shelf outside.

The surface layer is generated by the river input at the head of the fjord.

The low-saline surface water is pushed out of the fjord due to the density difference. The strongest velocity is found near the surface. On the interface between the water masses is a strong velocity shear, resulting in wave formation and breaking causing salty water being mixed into the surface layer. Because of this entrainment the total volume of the surface layer increases towards the mouth, together with increasing salinity. The total amount of water being entrained is depending on the energy available for mixing, mainly supported by the wind stress and tidal energy. Due to continuity a return flow is set up in the intermediate layer, compensating for the outflow in the upper layer. These processes are included in the estuarine circulation. The ventilation of the deep water is another circulation, controlled by vertical mixing and periodic overflows. When the sill depth is large and the intermediate layer is deep, the interaction between the estuarine circulation and deep water ventilation is weak (Stigebrandt, 1981).

The seasonal variations in fresh water input cause seasonal changes in the estuarine circulation. When the runoff increases during spring the estuarine circulation starts to develop, reaching maximum intensity in mid summer and then slowly reducing. During fall the stability of the water column is decreasing due to diminishing fresh water flux and cooling of the upper layer.

The interannual variability in fresh water input is also significant (see Figure 4.2), and is known to be correlated with the NAO-index[1] (Ottersen *et al.*, 2001). A high NAO-index causes high temperatures and enhanced precipitation mainly during winter season. These factors might give large interannual differences in the estuarine circulation, like earlier onset of melting season and increased runoff during winter.

3.1.1 Rotation

When movement is slow enough or on a sufficiently large scale, the rotation of the Earth starts to deflect the motion. This is a fictional force called Coriolis force and turns motion to the right in the northern hemisphere. In fjords the rotation starts to become important when the width is comparable to the internal Rossby radius for a two-layer system:

$$R = \frac{\sqrt{g' h_1}}{f} \tag{3.1}$$

where

$$g' = g\frac{\rho_2 - \rho_1}{\rho_2} \tag{3.2}$$

[1] The North Atlantic Oscillation winter index - a measure of the intensity of low-pressure systems in the North Atlantic

is the reduced gravity, f is the coriolis parameter, h_1 is the depth of the upper layer and ρ_1 and ρ_2 are the densities in the upper and lower layer, respectively. This formulae states that the internal Rossby radius is proportional to the density difference, which means that when the stratification is strong, then the rotation is less important. Since the stratification varies seasonally and interannually, the influence of rotation will also change significantly.

3.2 The vertical distribution of eggs

The Arcto-Norwegian Cod (ANC) spend most of their lives in the Barents Sea, but migrates towards the Norwegian coast for spawning. The spawning takes place at separate places along the coast, with the Lofoten area as the main spawning site (Sundby & Bratland, 1987). The spawning starts in the beginning of March, and continues until the beginning of May with a peek concentration around the first days of April (Ellertsen *et al.*, 1989). The Norwegian Coastal Cod (CC) are more stationary and mainly observed in coastal and fjord areas. The feeding areas are therefore closer to the spawning areas, which are located several places along the coast. The CC spawn during a longer time period than ANC, with a peek concentration 3-4 weeks later (Kjesbu, 1988).

Solemdal and Sundby (1981) collected ANC eggs in Lofoten from 1968 to 1972. They found the neutral buoyancy of the eggs, equivalent to salinity to be between 29.5 and 33.0 (see Figure 3.2). Within Vestfjorden these eggs are lighter than the surrounding water, resulting in a pelagic[2] distribution. Stenevik *et al.* (2008) measured specific gravity of eggs from the CC at several places along the Norwegian coast. They found that the buoyancy did not vary much between the locations, except for the northern most which is thought to be influenced by the ANC. In Tysfjord, at the inner part of Vestfjorden, the neutral buoyancy equivalent to salinity was ranging from 30.6 to 34.1 (see Figure 3.2). Which is slightly higher than the ANC eggs, causing a fraction of the CC eggs to be heavier than the surrounding water and being mesopelagically[3] distributed.

The vertical distribution of eggs is a function of ascending speed and downward mixing. The vertical velocity is given by Stokes' formulae:

$$w = \frac{1}{18}\frac{gd^2 \triangle \rho}{\mu} \tag{3.3}$$

[2]Pelagic eggs have a specific density lower than the mixed layer, Sundby (1991)

[3]Mesopelagic eggs have a specific density higher than the mixed layer and lower than the bottom layer, named bathypelagic eggs by Sundby (1991)

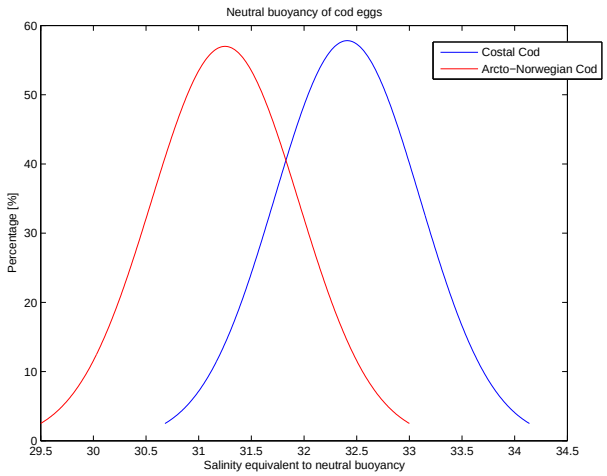

Figure 3.2: Neutral buoyancy of Arcto-Norwegian Cod (Solemdal and Sundby, 1981) and Norwegian Coastal Cod eggs (Stenevik *et al.*, 2008).

where g is acceleration due to gravity, d is diameter of the egg, $\triangle\rho = \rho_w - \rho_e$ is the density difference between the surrounding water and the egg and μ is molecular viscosity. The Stokes' formulae is only valid when the Reynolds number is low, Re < 0.5:

$$Re = \frac{\rho_w dw}{\mu} \tag{3.4}$$

Mixing can be supported by winds, tides and velocity shear. The pelagic eggs are mostly situated in the mixed layer and highly affected by wind-induced mixing (Sundby, 1983). Strong winds results in reduced concentrations at the surface and calm winds increase the surface concentration. The mesopelagic eggs are less affected by the winds and the vertical distribution has stronger dependency on buoyancy variations and stratification (Sundby, 1991).

Chapter 4

Model and methods

4.1 Fresh water discharge

Fresh water discharge is the major driving mechanism in fjords, controlling both the circulation and the hydrography (Sælen, 1967). In this chapter the annual mean discharge to the area is calculated and included in the circulation model.

When calculating the annual mean discharge, the area was divided into 17 drainage areas, see Figure 4.1. A planimeter was used on an isohydate-

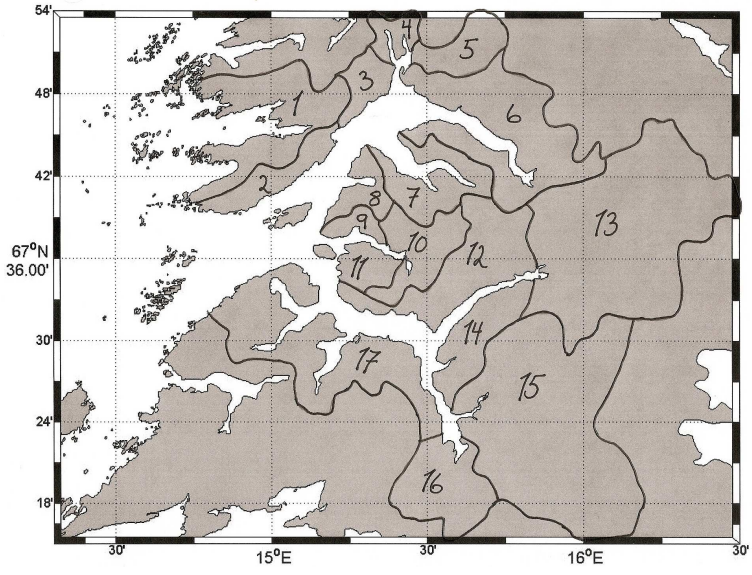

Figure 4.1: The 17 drainage areas in the fjord system.

map from NVE (The Norwegian Water Resources and Energy Directorate) to calculate the annual mean discharge in every of the 17 subregions, the results are shown in Table 4.1.

Table 4.1: Annual mean runoff for the period 1961-1990.

Drainage area	**m^3/s**	**Regime**	**Watermark**
1	7,66	coastal	Strandå
2	0,97	inland/transition	Lakså bridge
3	2,71	inland/transition	Lakså bridge
4	1,29	inland/transition	Lakså bridge
5	5,14	inland/transition	Lakså bridge
6	14,70	inland/transition	Lakså bridge
7	6,57	inland/transition	Lakså bridge
8	2,06	inland/transition	Lakså bridge
9	0,57	inland/transition	Lakså bridge
10	3,53	inland/transition	Lakså bridge
11	1,42	inland/transition	Lakså bridge
12	7,72	inland/transition	Vallvatn
13	42,76	mountain/glacier	Lakshola
14	4,89	inland/transition	Vallvatn
15	39,14	mountain/glacier	Lakshola
16	6,46	inland/transition	Vallvatn
17	11,87	inland/transition	Vallvatn
Total	159,46		

The drainage areas were classified in different regimes depending on elevation above sea level and distance from the coast (NVE, 2002). A coastal regime dominates near the mouth of the fjord system where the highest runoff is in autumn and winter and at a minimum in summer, highly depending on the precipitation. A mountain/glacier-regime is situated close to the head of the fjord, with high flows in the summer and low flows in winter due to retention of precipitation. Between these two is the inland/transition-regime with high runoff during spring and autumn and low flow during summer and winter. To include both information about annual mean discharge and seasonal variations a representative watermark had to be determined for every drainage area. NVE (Ingeborg Kleivane, pers.comm.) provided data from rivers in the area that could be used as watermarks. One watermark was selected to represent every regime (Table 4.2). For inland/transition-regime, two different watermarks was used, Lakså bridge in Nordfolda and Vallvatn

in Sørfolda. Information about the watermarks are found in Table 4.2, including some notes regarding the quality. The data are averaged over five days.

Table 4.2: Information about the watermarks in Folda, the location can be found in Figure 2.2.

Watermark	Time series	Regime	Notes
Lakså bridge	1953-2006	transition	
Lakshola	1916-2005	mountain/glacier	regulated after 1999
Strandå	1916-2007	coastal	poor data quality
Vallvatn	1953-2005	transition	low altitude

The data from the watermarks and the annual mean discharge are combined, and included into the model domain at the positions of the major rivers. The river runoff is released into the model area distributed over a number of grid cells in the horizontal depending on the size of the source. In the vertical the output is distributed over the 10 upper sigma layers, increasing towards the surface.

The annual mean discharge from the watermarks (Table 4.2) is shown in Figure 4.2. The data have been standardized for comparison. The different

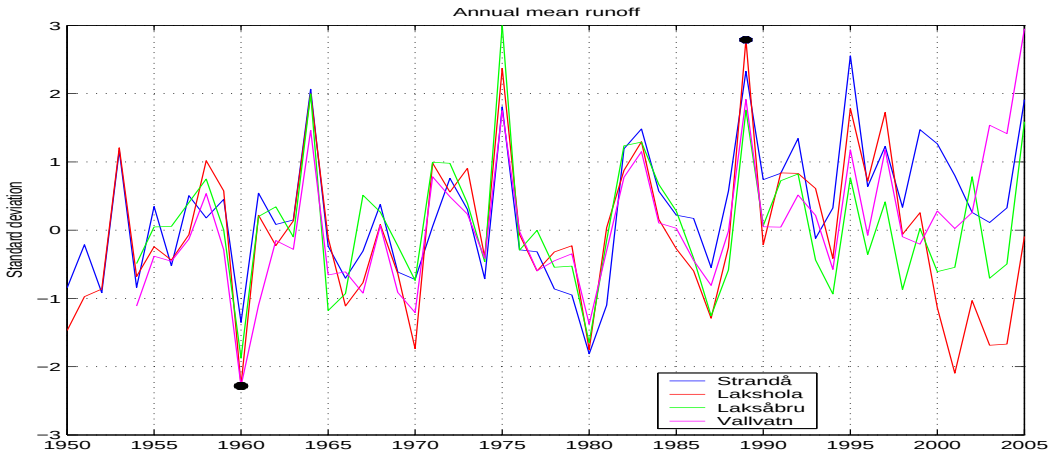

Figure 4.2: The annual mean discharge for all watermarks, standardized for comparison. The two selected years are marked with black circles.

watermarks show similar interannual variability, except after 1999. In 1999 Lakshola was regulated, which had a major impact on the annual mean

discharge. From this data the two years, 1960 and 1989, were chosen. Both years are more than two standard deviations away from the mean, in opposite directions.

Figure 4.3 shows the seasonal variations of discharge for all the watermarks. The upper panel shows the data from Lakshola during 1960 and

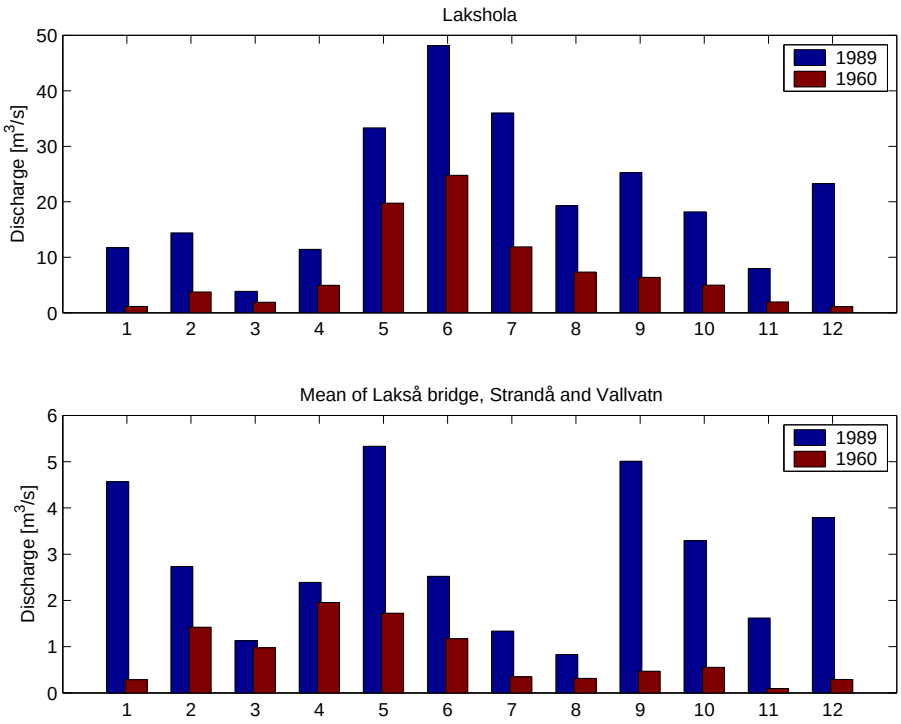

Figure 4.3: Monthly mean discharge for the years 1960 and 1989, note different scales.

1989, whereas the lower panel shows the mean from Lakså bridge, Strandå and Vallvatn (note different scales). It is clear that Lakshola is the dominating fresh water source in the area, approximately 10 times larger then the others (see also Table 4.1). Lakshola is representing a mountain/glacier regime, with a clear summer maximum discharge. In 1989 the summer maximum was twice as large as in 1960. Lakså bridge, Vallvatn and Strandå represent an inland/transition and a coastal regime. The major difference between these watermarks and Lakshola is the enhanced discharge during fall (September and October) and winter (December and January), most pronounced in 1989. All months show higher runoff through 1989 than 1960.

The spawning takes place in the spring time, with a peek concentration in April. Figure 4.3 shows that the discharge during this period is about twice

as large in 1989 than in 1960 for Lakshola. For the watermarks Lakså bridge, Strandå and Vallvatn the difference between 1989 and 1960 is not so great in March and April, but much larger in May. Lakshola shows a strong increase in runoff during the spring months, from about 5 m^3/s in March to above 30 m^3/s in May. The other watermarks show an increase only during spring 1989. This means that the spring is a major transient time. A shift in the seasonal cycle of discharge would have a large impact on the runoff during this period. Changes in fresh water input during spring coincides with the spawning and may affect the transport of eggs.

In 1968 a major fresh water source at the inner end of Sørfolda was regulated. This is not included in these calculations. The regulation caused water to be guided away from drainage area 15 to 16, which caused a change in the annual mean runoff. The seasonal variations are also expected to be altered, with increased runoff during winter and reducing the maximum flow.

4.2 The circulation model

The model used for these simulations is the Regional Ocean Modeling System (ROMS) version 3.0, algorithms described by Shchepetkin and McWilliams (2005). This is a free-surface, hydrostatic, primitive equation ocean model that uses stretched terrain-following s-coordinates in the vertical and curvilinear coordinates in the horizontal (Haidvogel *et al.*, 2007). The primitive equations are solved by the finite differences method on an Arakawa C-grid, including a Generic Length Scale (GLS) turbulence closure scheme (Umlauf & Burchard, 2003).

The model domain is shown in Figure 4.4. The high resolution bathymetry was obtained from Statens Kartverk (Sjøkartverket) and included in Figure 4.4. In the actual model run the largest depth was set to 300 m, and the bathymetry was smoothed around steep slopes. The grid is rotated with an angle of 45° relative to the latitude, origo is positioned at longitude 15.15°E and latitude 67.24°N. The grid length is 200 m with 257 points in ξ direction and 282 points in η direction. In the vertical there are 35 sigma layers, close together near the surface and reduced resolution in the lower layers and towards the bottom. Sigma layer number 35 is the surface layer. The resolution in the upper layers varies from 0.29 m to 0.33 m, and at the bottom from 2.1 m to 53.5 m. The baroclinic timestep is 60 seconds, with 60 barotropic time steps between each baroclinic timestep.

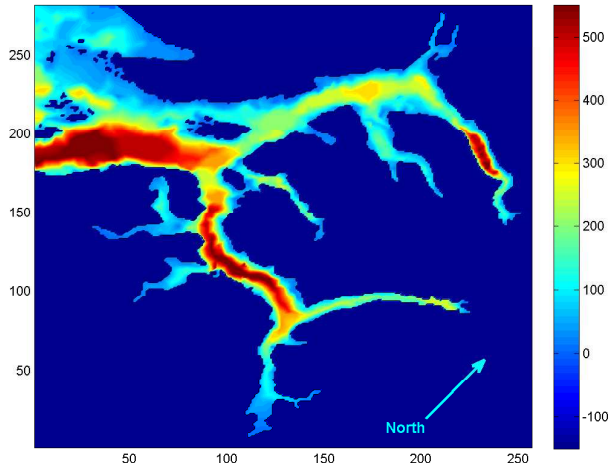

Figure 4.4: The model domain including bathymetry, with horizontal axes ξ (u direction) and η (v direction).

4.2.1 The governing equations

The primitive equations solved by ROMS are presented in Cartesian coordinates:

$$\frac{\partial u}{\partial t} + \vec{v} \cdot \nabla u - fv = -\frac{1}{\rho_0}\frac{\partial p}{\partial x} + F_u + D_u \tag{4.1}$$

$$\frac{\partial v}{\partial t} + \vec{v} \cdot \nabla v + fu = -\frac{1}{\rho_0}\frac{\partial p}{\partial y} + F_v + D_v \tag{4.2}$$

assuming the Boussinesq approximation[1]. The variables are explained in the Table 4.3. Further, the hydrostatic approximation is applied, assuming the vertical pressure gradient balances the buoyancy force:

$$\frac{\partial p}{\partial z} = -\rho g \tag{4.3}$$

The equation of continuity for an incompressible fluid is given by:

$$\frac{\partial u}{\partial x} + \frac{\partial v}{\partial y} + \frac{\partial w}{\partial z} = 0 \tag{4.4}$$

The time evolution of the potential temperature and salinity fields are governed by the advective-diffusive equations:

$$\frac{\partial T}{\partial t} + \vec{v} \cdot \nabla T = F_T + D_T \tag{4.5}$$

[1]Boussinesq approximation - density differences are neglected except in the vertical when contributing to the buoyancy force

$$\frac{\partial S}{\partial t} + \vec{v} \cdot \nabla S = F_S + D_S \tag{4.6}$$

The density field is computed according to the equation of state:

$$\rho = \rho(T, S, P) \tag{4.7}$$

Table 4.3: Description of the variables used in the equations above.

D_u, D_v, D_T, D_S	diffusive terms
F_u, F_v, F_T, F_S	forcing terms
f	Coriolis parameter
g	acceleration due to gravity
P	total pressure $P \approx -\rho_0 g z$
$\rho_0 + \rho(x, y, z, t)$	total *in situ* density
$S(x, y, z, t)$	salinity
$T(x, y, z, t)$	potential temperature
t	time
u, v, w	the (x, y, z) components of vector velocity $\vec{v}$
x, y	horizontal coordinates
z	vertical coordinate

4.2.2 Initial field

The initial field was calculated from data collected in Folda November 1993, a year with near average runoff conditions. The fjord system was divided into three regions: Nordfolda, Sørfolda and the mouth area. One profile representing each area was selected and smoothed out to cover the whole fjord system. Linear interpolation was used to nest everything together. This initial field was used in all simulations.

4.2.3 Forcing

All atmospheric forcing was extracted from the ERA40 archive, with a horizontal resolution of 1 degree. This includes cloud cover, air pressure, specific humidity, precipitation, air temperature and wind components. All variables are obtained every sixth hour.

The boundary conditions are taken from a dataset covering the Nordic Seas (Engedahl *et al.*, 1998), containing salinity, temperature, currents and surface elevation. The data are monthly means based on several years of

observations and model output. This forcing will be included along the open boundaries, and is equal in all simulations.

Three semi-diurnal tidal components (M_2, S_2, N_2) and one diurnal component (K_1) are added along the open boundaries (Moe *et al.*, 2002). The lateral boundary conditions are implemented using a combination of Flather (Flather, 1976), Chapman (Chapman, 1985) and flow relaxation scheme (Martinsen & Engedahl, 1987).

The fresh water forcing is described in section 4.1

4.2.4 Model run

After studying the variations in annual mean discharge (see Figure 4.2), the years 1960 and 1989 were selected to be further investigated. The reason is that 1960 represents a cold and dry year, and 1989 a warm and wet year. The impact of variations in annual mean discharge can then be studied.

In the different runs the initial field, the climatology and the tidal forcing will be the same. The differences are in atmospheric forcing and runoff. The simulations start 1^{st} November 1959 and 1988, because of the data used in the initial field, and continue until 31^{st} December without wind forcing. Then the wind is included and the model runs continue until 31^{st} May 1960 and 1989. This was done because of the need for shorter time steps when the wind forcing is included.

4.3 The particle tracking model

A Lagrangian Advection and DIffusion Model (LADIM) is used to simulate transport of eggs (Ådlandsvik & Sundby, 1994). The model uses the saved output from ROMS to advect the eggs with the currents. In the simplest case the eggs are held at a constant depth and transported around for a time period. For a more realistic case the eggs are allowed to be displaced vertically, resulting in a dynamical vertical distribution. Each egg has its own specific gravity and a vertical velocity is calculated depending on the density difference between the egg and the surrounding water. Then the vertical dispersal is calculated with the finite-volume method and binned random walks (Thygesen & Ådlandsvik, 2007). Totally 100 bins are used with a distance of 1 m, which means that particles cannot go deeper than 100 m. The model only calculates within which bin the particle is located, hence with a vertical resolution of 1 m.

Chapter 5

Model results

This chapter includes the main results from the two model runs. First an overview of the salinity distribution in the whole fjord system is given, on 10^{th} April and 25^{th} April in 1960 and 1989. Then the circulation pattern in the mouth area is shown on the same dates, in Figure 5.2 and 5.3. Cross-sections from the sill in Sørfolda and Nordfolda are then presented (Figure 5.6 and 5.7). Section 5.4 displays vertical profiles at different locations in the fjord, followed by temporal variations in the vertical structure. The next section shows the monthly mean salinity and temperature profile during the spring. In the last section the circulation and salinity at the mouth of Leirfjorden are shown, during a 5-days transition period in April 1989.

The hydrography and circulation inside the fjord system are important for the spreading and distribution of cod eggs. As mentioned in section 3.2, the vertical velocity of eggs is a function of the density difference between the eggs and the surrounding water. Hence, changes in the hydrography will change the vertical distribution of eggs in the water column. The estuarine circulation inside a fjord is characterized by strong vertical gradients in the current field, see section 3.1. A vertical movement of the eggs might cause them to enter the outflowing surface layer or the inflow at the lower levels.

5.1 Salinity distribution

Figure 5.1 shows the salinity at 1 m depth in Sørfolda and Nordfolda. The data from 10^{th} April and 25^{th} April are shown in both 1960 and 1989, all with same scales. This is about the same time as the spawning occurs, and when the fresh water discharge is increasing.

Figures 5.1(a) and 5.1(b) are from 10^{th} April 1960 and 1989, respectively. The freshest areas in 1960 are at the inner end of the fjord. The salinity is

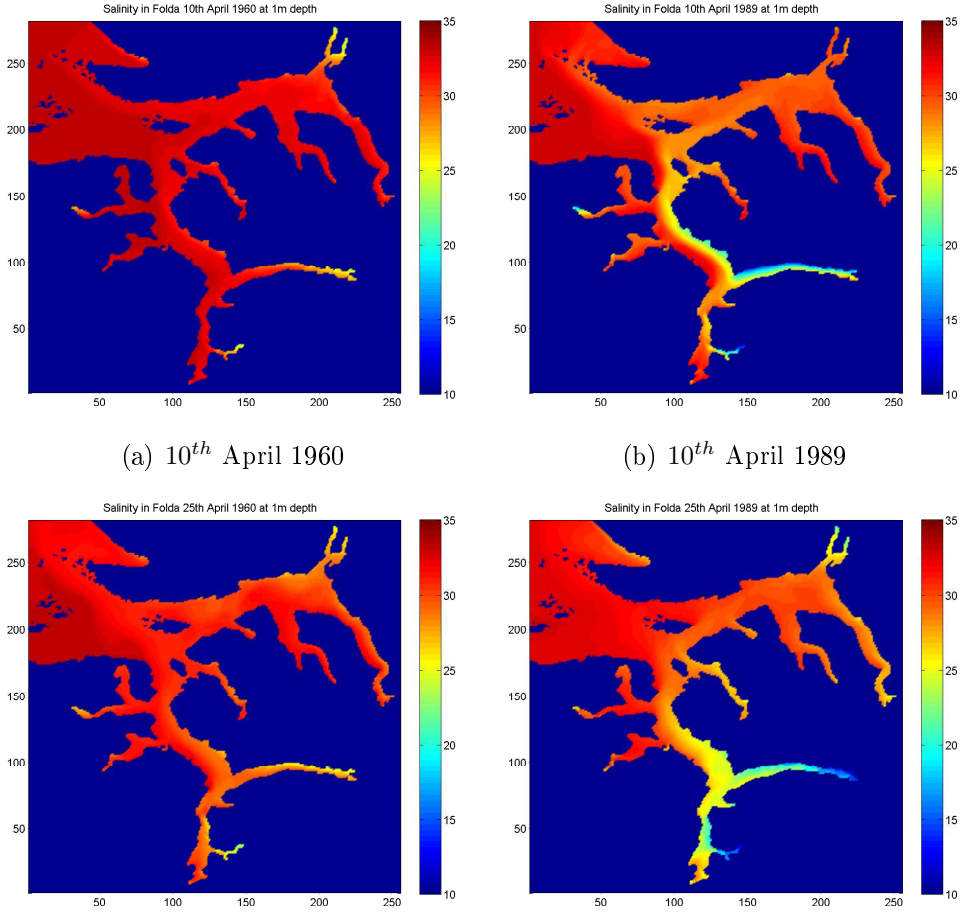

(a) 10^{th} April 1960

(b) 10^{th} April 1989

(c) 25^{th} April 1960

(d) 25^{th} April 1989

Figure 5.1: Salinity at 1 m depth.

slightly lower in Nordfolda (∼32) than in Sørfolda (∼33), but generally the horizontal variations are small. Leirfjorden is the freshest fjord area in 1989, however a few other branches show very low salinity at the head. There are very small cross-fjord variations inside Leirfjorden, but in Sørfolda the fresh surface layer is constricted to the right hand side, in relation to the flow directions, causing strong cross-fjord variance. In Nordfolda the salinity is quite constant in the whole fjord. Brackish water leave the fjord on the northern side of the mouth area. When comparing 1960 and 1989, the main difference is the distinct low-saline water in 1989 located in Leirfjorden and Sørfolda. The salinity is in general lower during 1989 than 1960 for the whole fjord system. The cross-fjord variability is significantly larger in 1989 as well.

Figures 5.1(c) and 5.1(d) are from the same area 15 days later in spring, 25^{th} of April. The salinity is in general lower on 25^{th} April than on 10^{th} April for the entire area. Both years show a progressively increasing salinity from head to mouth in all fjord branches. Some cross-fjord variability is observed in Sørfolda, most distinct in 1989. Both years show brackish water on the northern side of the mouth. The salinity in 1960 is on average higher than in 1989. On 25^{th} April 1989 a difference between Sørfolda and Nordfolda is observed, with lowest salinity in Sørfolda. This shift in salinity correlates to the difference in fresh water input to Nordfolda and Sørfolda, as discussed in section 2.2.

5.2 Circulation pattern in mouth area

The estuarine circulation develops in both fjords for both model runs, 1960 and 1989. The circulation is then characterized by an outflow in the upper layer and a compensating inflow below.

The circulation pattern in the mouth area can be quite complicated. The currents have strong variability depending on density differences, winds and tides. This is also where Nordfolda and Sørfolda interact with each other and with the shelf areas. The amount of exchange between these two fjords will affect the horizontal distribution of cod eggs.

5.2.1 Circulation on 10^{th} April

Figure 5.2 shows the circulation in the mouth area at 1 m depth on 10^{th} April 1960 and 1989, the same time as 5.1(a) and 5.1(b). Both years show an outflow from Sørfolda, strongest in 1989 (note different scales). In 1960 a large part of the current is turning towards Nordfolda, and joining a westerly flow north of the island Hjartøy leaving the fjord system on the northern side of the mouth. In 1989 the outflow from Sørfolda is divided at Hjartøy with one branch entering Nordfolda and one branch leaving the area.

The Figures 5.3(a) and 5.3(b) show the currents at 10 m depth at the same time and place as before. The picture is more complicated at this depth. In 1960 there is still a small outflow from Sørfolda, but a stronger outflow from Nordfolda on the northern side of Hjartøy and leaving the area. On the southern side several eddies are seen where water masses from Nordfolda and Sørfolda meet. In 1989 the outflow from Sørfolda is weak, and a strong outflow from Nordfolda is spreading out on both sides of Hjartøy. There is a westerly current on the northern side of the mouth and a large eddy is situated further south. The circulation pattern in 20 m is not shown since it

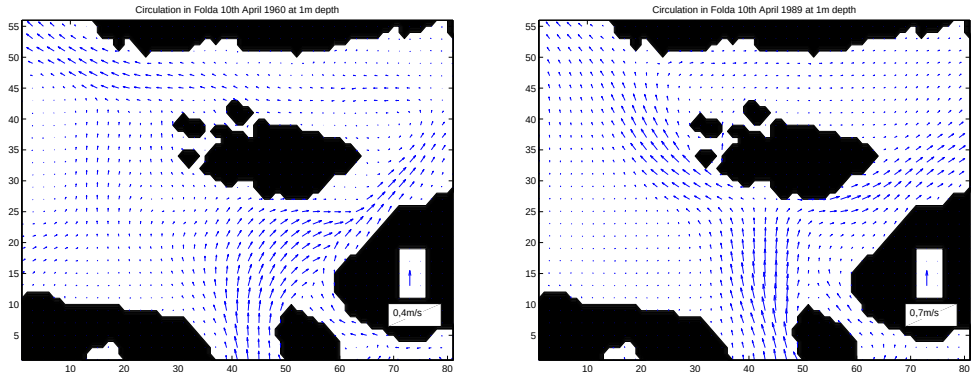

(a) 1960 at 1 m depth (b) 1989 at 1 m depth

Figure 5.2: Daily mean currents on 10^{th} April, covering the mouth area with Sørfolda at the south, Nordfolda to the east and opening to the west.

is similar to 10 m.

Figures 5.3(c) and 5.3(d) show the currents at 30 m depth at 10^{th} April. In this case there is an inflow towards Sørfolda in both years. In 1960 the inflow comes from Nordfolda and in 1989 from the mouth area. A large cyclonic eddy is located on the southern side of the opening in 1989, as was visible in 10 m. A weak outflow from Nordfolda is flowing on the southern side of the Hjartøy and entering the eddy.

5.2.2 Circulation on 25^{th} April

Figure 5.4 shows the circulation pattern at the mouth area on 25^{th} April 1960 and 1989, at the depths 1 m, 10 m and 30 m. The currents at 20 m is not shown because of strong similarities with 30 m depth.

At 1 m depth the current is directed out of Sørfolda in both years. In 1960 the outflow turns left and passes Hjartøy on the western side. However, in 1989 the outflow turns right and enters Nordfolda. An outflow from Nordfolda is visible at 10 m depth in 1960, flowing on the southern side of Hjartøy and entering the mouth area. In 1989 the outflow from Nordfolda at 10 m depth is deflected at Hjartøy, and no distinct pattern is visible elsewhere. The circulation at 30 m depth is quite complex and several eddies are seen. A week inflow into Sørfolda is seen in 1960 and an anticyclonic circulation around Hjartøy. A large cyclonic eddy is located in the mouth area. The currents are directed out of Sørfolda in 1989, with weaker velocities than in 1960.

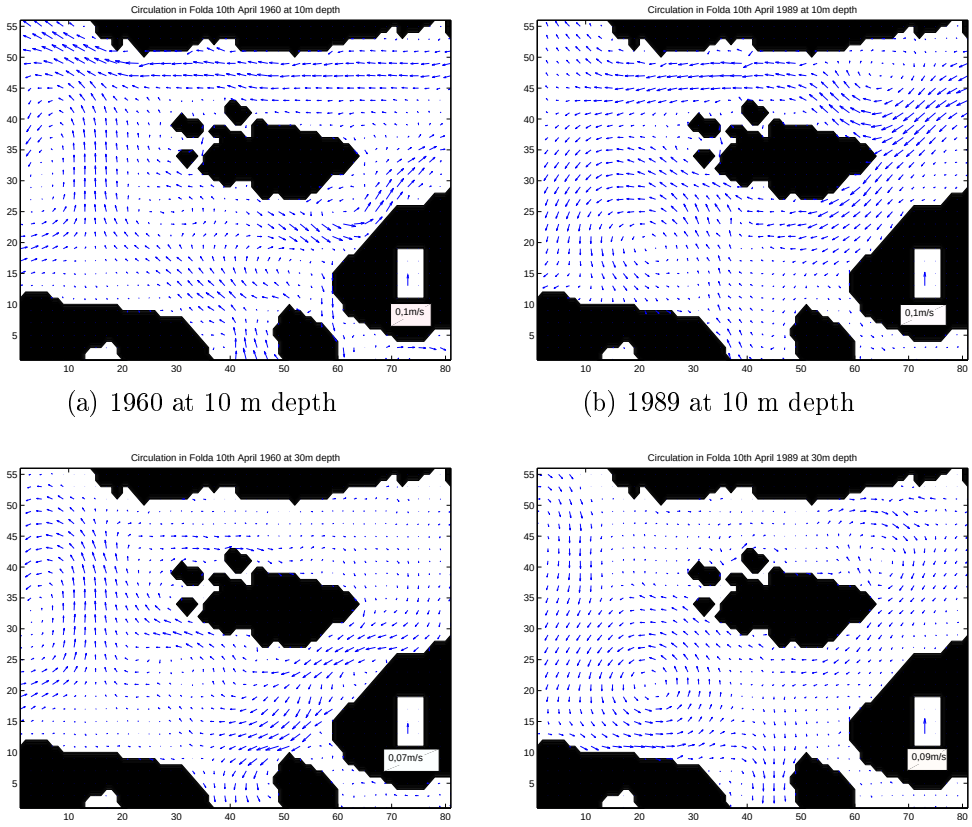

(a) 1960 at 10 m depth

(b) 1989 at 10 m depth

(c) 1960 at 30 m depth

(d) 1989 at 30 m depth

Figure 5.3: Daily mean currents at 10 m and 30 m depth on 10^{th} April.

The results shown here demonstrate that the circulation pattern in the mouth area changes between the two different dates, 10^{th} and 25^{th} April during both years. No particular situation can be recognized to represent each year. As mentioned earlier the currents in the mouth area are complicated and depend on the volume flux of brackish water, winds and tides. In periods with large fresh water input and weak winds the outflow from Sørfolda is most often observed to leave the fjord system on the western side of Hjartøy. When the freshwater discharge is lower and the outflow is weaker, the surface flow in Sørfolda is more likely to be directed into Nordfolda. The winds also have greater impact on the system when the brackish water fluxes are low.

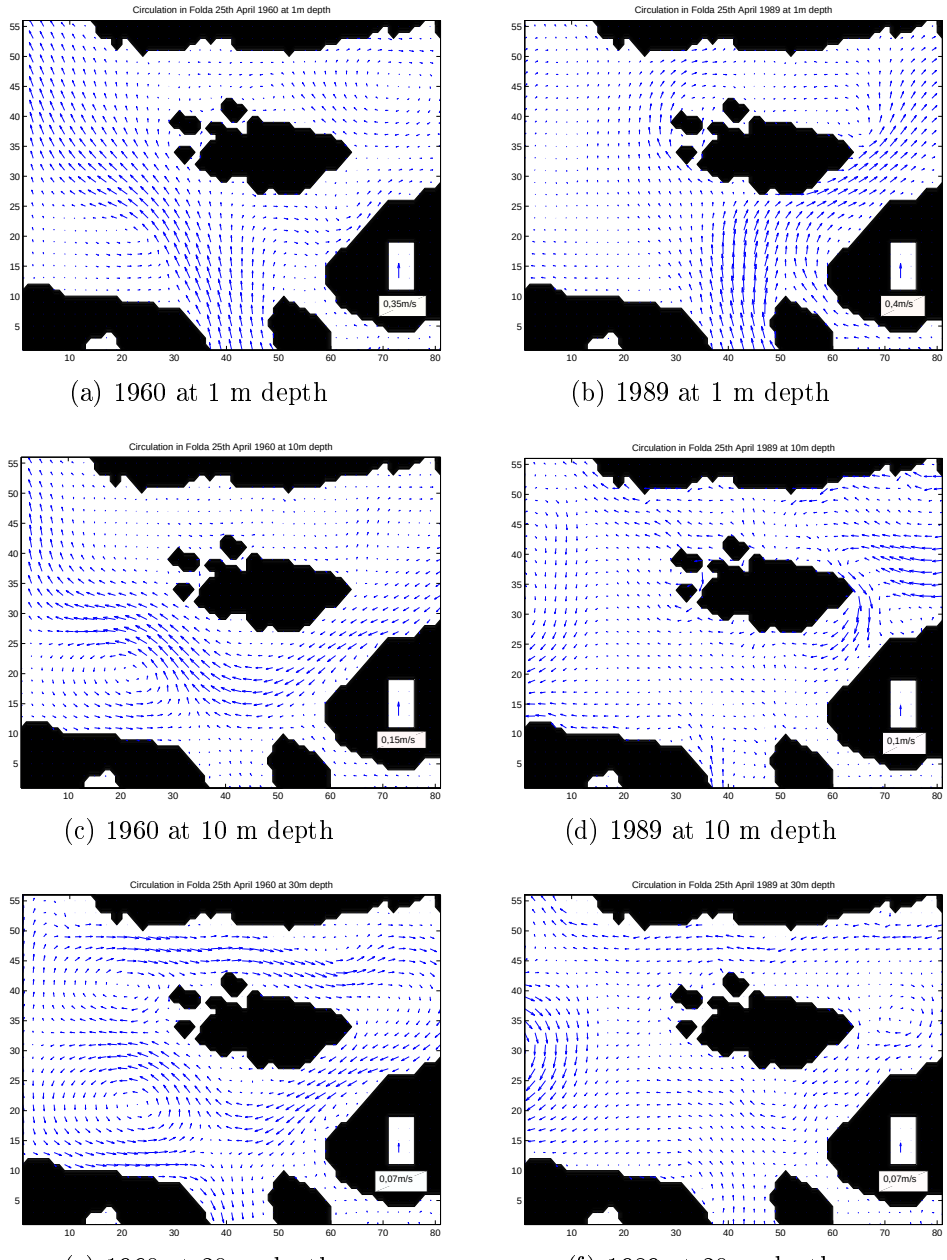

(a) 1960 at 1 m depth

(b) 1989 at 1 m depth

(c) 1960 at 10 m depth

(d) 1989 at 10 m depth

(e) 1960 at 30 m depth

(f) 1989 at 30 m depth

Figure 5.4: Daily mean currents on 25^{th} April, covering the mouth area.

5.2.3 Eddies

In a fjord system with large spacial variability in currents, the possibility for eddies to form is large. An eddy has the potential to induce strong turbulence and generate mixing. In a fjord system like Folda the eddy size is limited by the width of the fjord. In Sørfolda and Leirfjorden, which are narrow and have strong fresh water input, the production of eddies is limited. Only when the estuarine circulation is reversed small eddies form, see section 5.7. In the main part of Nordfolda the width is large enough and the fresh water flux is small enough for transient eddies to develop. However, the temporal and spatial variability is large, such that no distinct pattern can be described. In the mouth area the results indicate a cyclonic eddy situated west of Hjartøy, also highly varying in time. This eddy is visible in Figure 5.3 and Figure 5.4.

5.3 Cross-sections at the sill

Both main fjords, Sørfolda and Nordfolda, have a sill close to the mouth at 265 m and 225 m depth. A sill is a vertical constriction of the water column, which might cause reduced exchange between the fjord and the coastal areas.

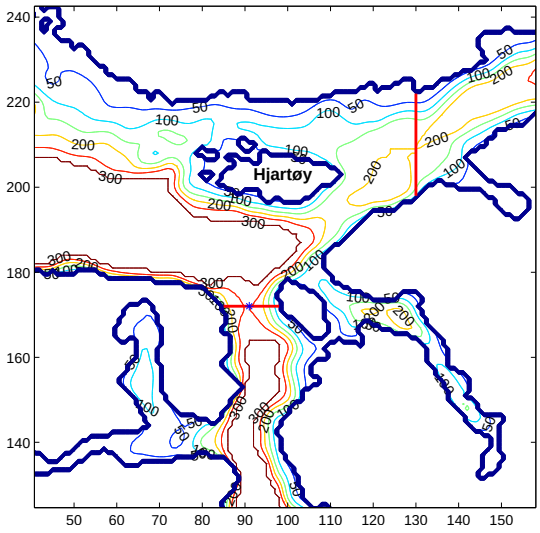

Figure 5.5: The cross-sections at the sill in Sørfolda and Nordfolda, marked as red lines.

5.3.1 At the sill in Sørfolda

Figure 5.6 shows cross-sections at the sill in Sørfolda on 10^{th} April 1960 and 1989, at the position shown in Figure 5.5. The current speed and the salinity structure from 1960 are seen in 5.6(a) and 5.6(b). Positive current velocity is directed out of the fjord. The largest current speed is observed in the surface layer. The depth of no motion is lower on the eastern side than on the western side. The current is directed in the opposite way below 25 m, going into the fjord. The salinity structure shows freshest water in the upper layers on the eastern side.

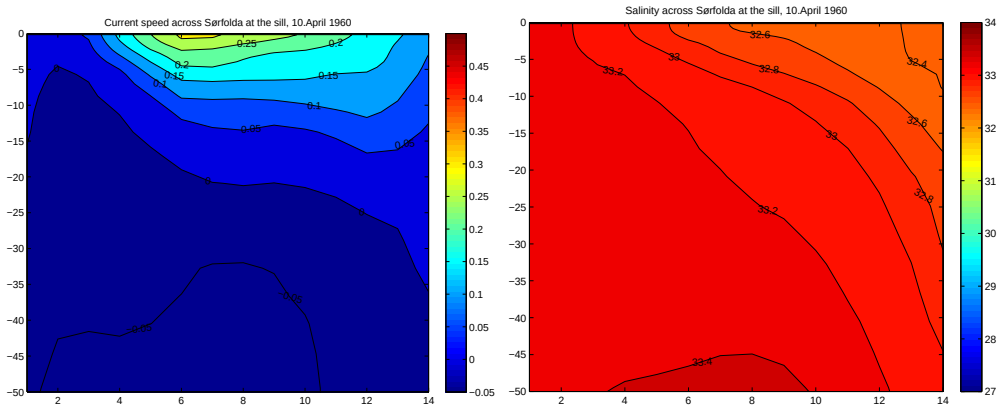

(a) Current speed 1960 (b) Salinity 1960

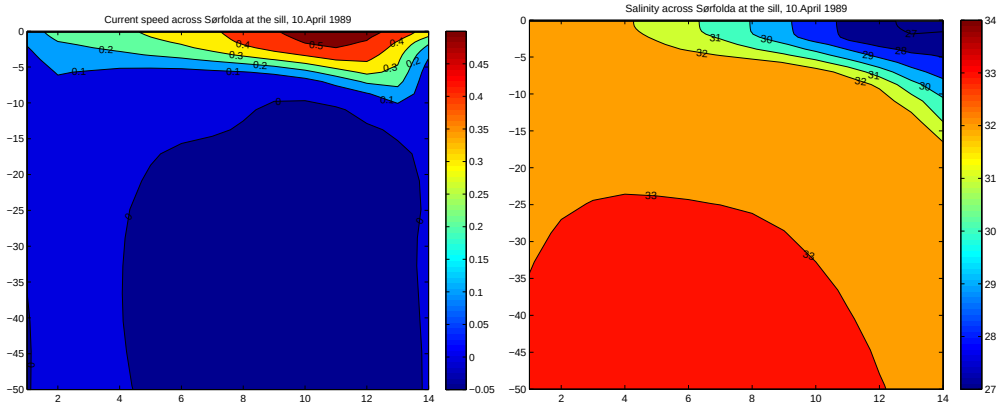

(c) Current speed 1989 (d) Salinity 1989

Figure 5.6: Cross-sections at the sill in Sørfolda 10^{th} April, from west to east. Positive current velocity is directed out of the fjord and the x-axis is number of grid points.

The Figures 5.6(c) and 5.6(d) are showing current speed and salinity on

10^{th} April 1989. The strongest current speed is seen in the upper layers, constricted to the upper 5 m. The strength of the current is greater in 1989 than compared to 1960. The salinity profile shows a fresh surface layer on the eastern side. The stratification is weak on the western side of the fjord .

5.3.2 At the sill in Nordfolda

Figure 5.7 displays cross-sections at the sill in Nordfolda on 10^{th} April 1960 and 1989, at the position shown in Figure 5.5.

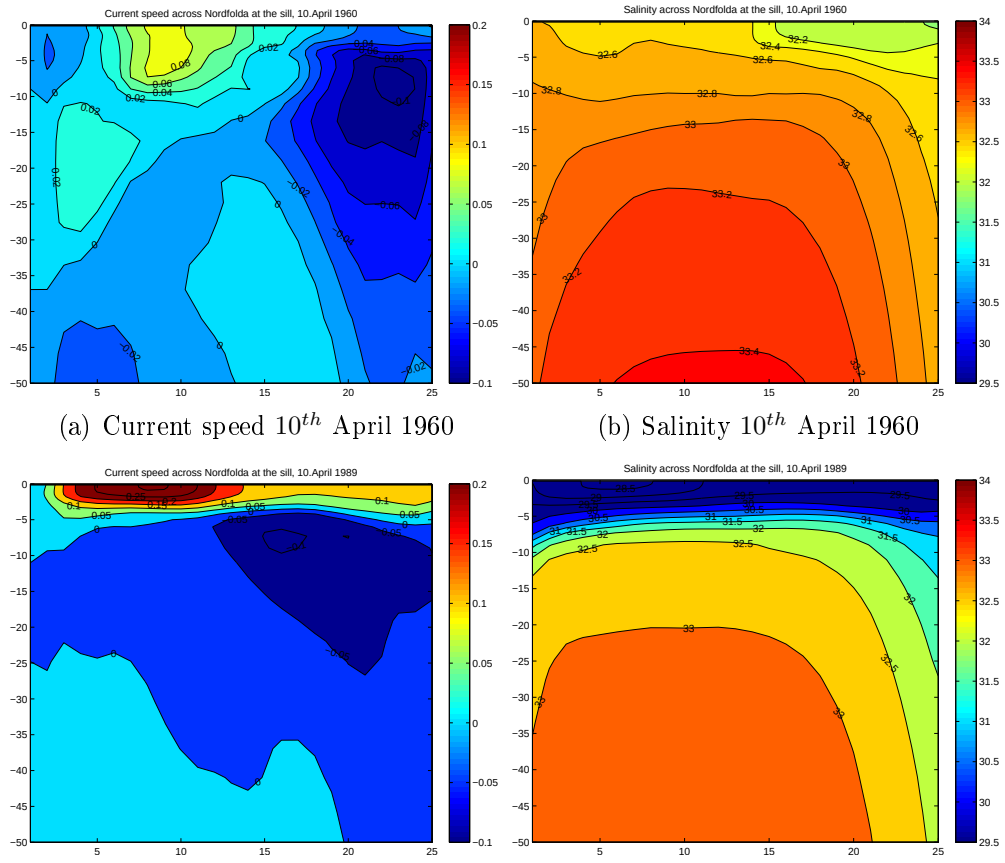

(a) Current speed 10^{th} April 1960

(b) Salinity 10^{th} April 1960

(c) Current speed 10^{th} April 1989

(d) Salinity 10^{th} April 1989

Figure 5.7: Cross-sections at the sill in Nordfolda, from south to north. Negative current velocity is directed out of the fjord and the x-axis is number of grid points.

The Figures 5.7(a) and 5.7(b) show the salinity structure and current speed on 10^{th} April 1960. Negative current speed is directed out of the fjord.

An outflow is observed on the northern side, concentrated between 5 m and 20 m depth. Towards the southern side of the fjord is an inflow in the upper 10 m. The salinity distribution shows a stratification, with freshest (<32.2) water on the northern side.

The lower panels (5.7(c) and 5.7(d)) display the same section from 10^{th} April 1989. An outflow is seen below about 5 m, strongest on the northern side of the fjord between 5 m and 25 m. An inflow is observed in the upper 5 m, reaching 0.3 m/s on the southern side. The salinity profiles show a strong stratification, where the surface salinity is close to 28.5. Above 5 m the freshest water is located on the southern side, below 10 m the low-saline water is situated on the northern side. When comparing with Figure 5.2(b), the reason for the inflow and low-saline water in Nordfolda is explained by the outflow from Sørfolda turning towards Nordfolda.

5.4 Spatial variability in vertical structure

Figure 5.8 shows the vertical profiles of salinity and the along-fjord current velocity on 10^{th} April 1960, at four different locations in the fjord system. The positions are shown in Figure 2.2 as blue boxes and red stars, located in Sørfolda, Leirfjorden, Nordfolda and in the mouth area.

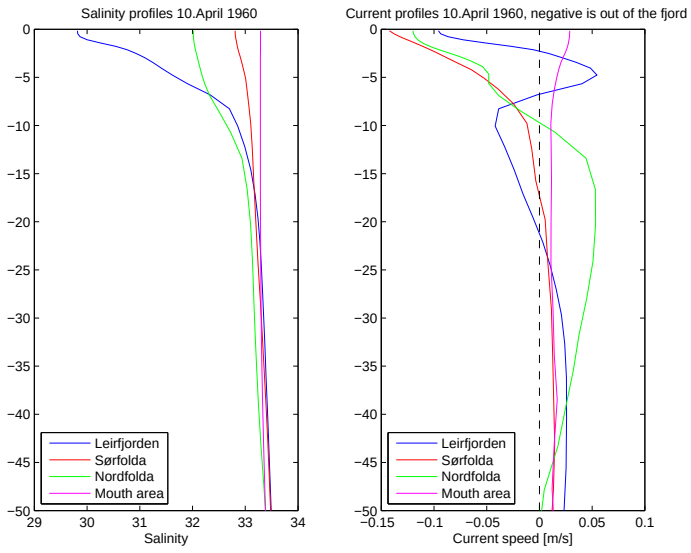

Figure 5.8: Vertical profiles of salinity (left) and along-fjord current velocity (right) at four different locations in the fjord system on 10^{th} April 1960, positions shown in Figure 2.2.

The freshest (<30) surface layer is observed in Leirfjorden. In Nordfolda the surface salinity is about 32, and just below 33 in Sørfolda and above 33 at the mouth. There is a strong outflow in Sørfolda, Nordfolda and Leirfjorden and a weak inflow at the mouth area in the surface layer. In Sørfolda the current reduces with depth, reaching inflow below 20 m. The current in Leirfjorden decreases rapidly and becomes positive between about 3 m and 8 m. Around 10 m depth there is an outflow, and below 20 m an inflow is seen. The current in Nordfolda is directed outwards above 10 m, with a maximum at the surface, and a relatively strong inflow between 10 m and 50 m. At the mouth a constantly weak inflow at all depths is seen.

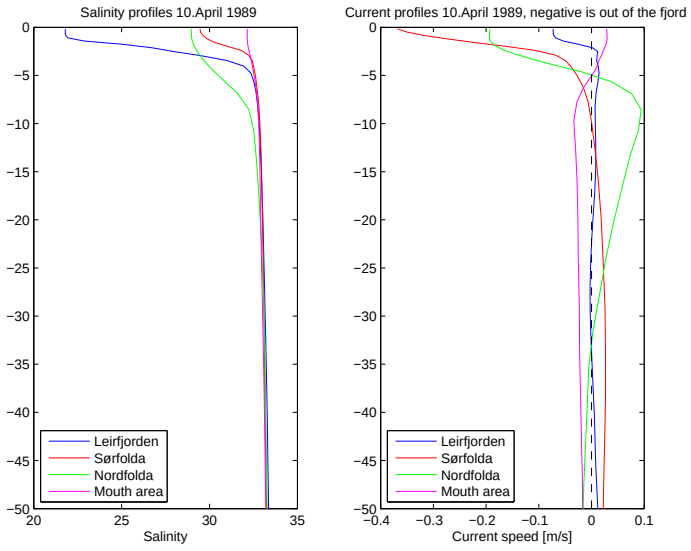

Figure 5.9: Vertical profiles of salinity (left) and horizontal current velocity (right) at four different locations in the fjord system on 10^{th} April 1989, positions shown in figure 2.2.

Figure 5.9 shows the same profiles from 10^{th} April 1989. The profiles show the same structures but the scales are larger. The surface salinity in Leirfjorden is now approximately 22 and the thickness of the surface layer is close to 3 m. In Nordfolda and Sørfolda the surface salinity is below 30. The surface layer is more distinct in 1989 than 1960 at all locations, except at the mouth area. The strongest surface current is located in Sørfolda (>0.3 m/s) and Nordfolda (0.2 m/s) going out of the fjord, compared with less than 0.15 m/s in 1960. In Nordfolda a strong inflow 5 m and 20 m is observed. A diffuse inflow is seen in Sørfolda and Leirfjorden in the lower layers. At the mouth the surface current is directed into the fjord, changing to opposite

direction at about 5 m depth.

5.5 Temporal variability in vertical structure

Figure 5.10 displays the salinity in the upper 50 m during March, April and May 1960 and 1989 at a station at the sill in Sørfolda. The position is marked as a blue star on the cross-section in Sørfolda in Figure 5.5. These figures illustrate the variability in the salinity, and the development of a surface layer in the fjord.

The upper panel (Figures 5.10(a) and 5.10(b)) shows the salinity through March 1960 and 1989. Both years show only small variations in the upper layers. The minimum surface salinity in 1989 ($\sim$32.5) is lower than in 1960 ($\sim$32.8). At 50 m depth the salinity is constant during the whole period.

Entering April (Figures 5.10(c) and 5.10(d)) the surface salinity shows larger variability than in March. At the end of April 1960 a distinct surface layer is created with a minimum salinity of 30. Below 15 m no variability is observed. Already in the beginning of April 1989 a low-saline surface layer is generated. This surface layer is about 5 m deep and has salinities down to 27. However, the existence of this upper layer is not constant. It disappears occasionally and the salinity varies between 27 and 33. Four different incidents of a well established surface layer are apparent. In the layers below it is seen that the 33-isohaline is rising, from about 30 m in the beginning of April to 15 m at the end.

Figures 5.10(e) and 5.10(f) show the salinity structure during May 1960 and 1989. There is a distinct surface layer through May 1960, with a depth of about 5 m. Two episodes of low surface salinity are apparent, with a minimum of 24. May 1989 shows a strong stratification through the whole period, with salinities down to 16. The depth of the surface layer varies between 5 m and 15 m. There are several incidents of low-saline surface water.

Figure 5.11 shows the in and outflow in the upper 50 m during March, April and May 1960 and 1989 at the sill in Sørfolda, with positive direction out of the fjord. The currents in the upper part are subjected to strong variability during the whole period.

The current speed during March 1960 and 1989 is shown in Figures 5.11(a) and 5.11(b). During March 1960 the current has small vertical variations, and has the same direction through out the upper 50 m. Two episodes of inflow are seen around 6^{th} and 20^{th} March, with maximum speed of 0.15 m/s. In between these two episodes is an incident of outflow.

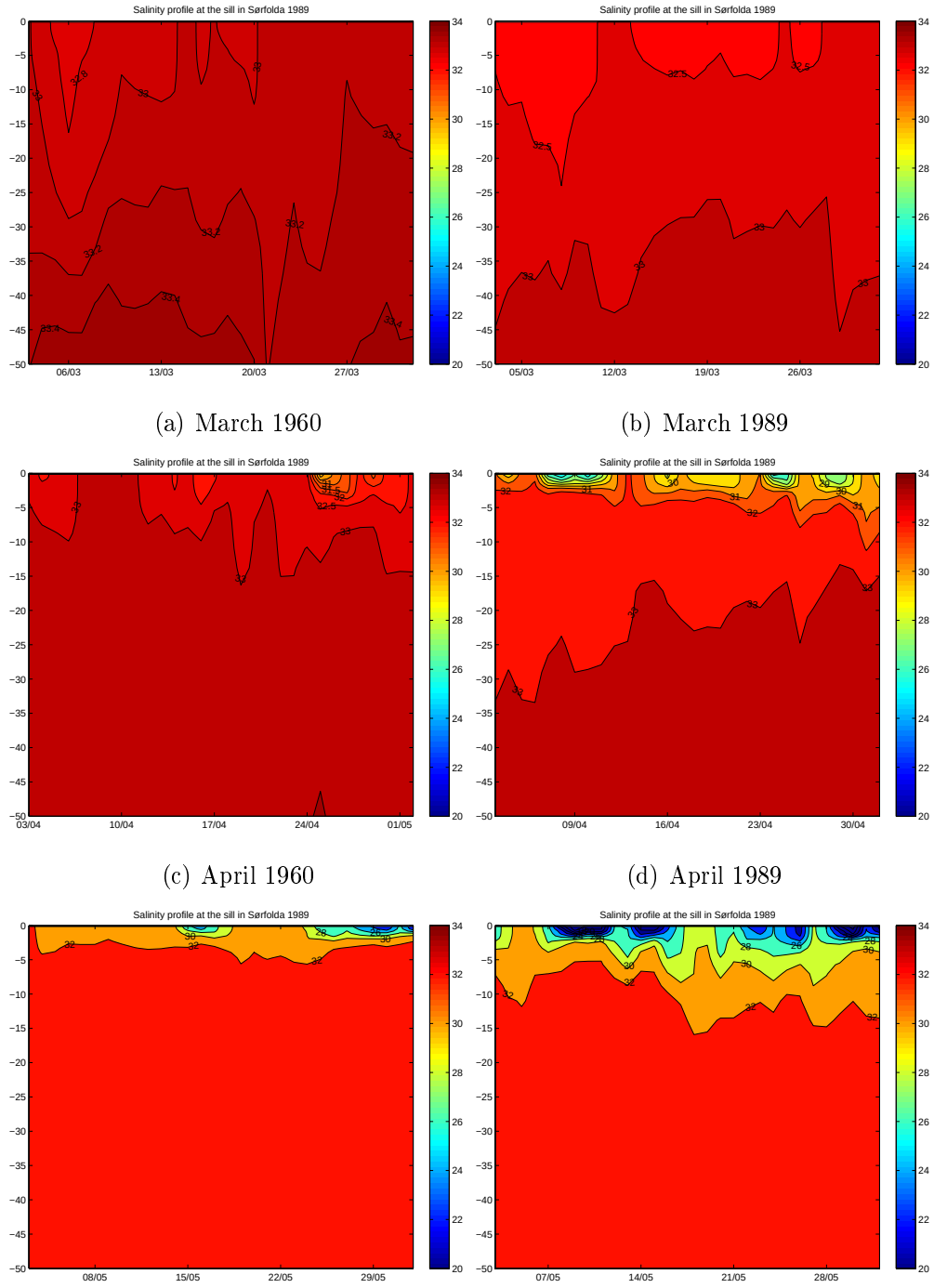

(a) March 1960 (b) March 1989

(c) April 1960 (d) April 1989

(e) May 1960 (f) May 1989

Figure 5.10: Salinity profile at the sill in Sørfolda in March, April and May.

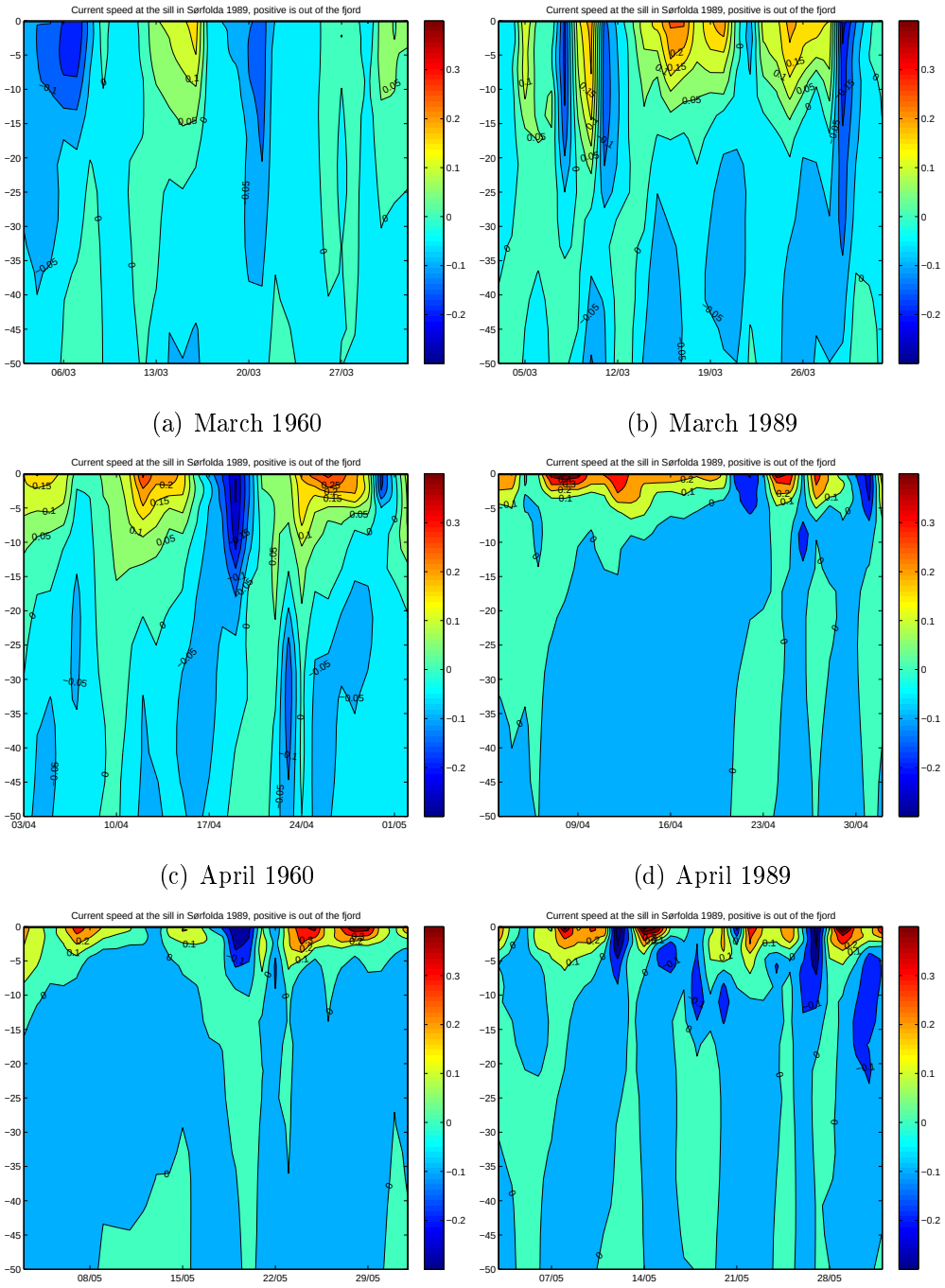

(a) March 1960

(b) March 1989

(c) April 1960

(d) April 1989

(e) May 1960

(f) May 1989

Figure 5.11: Horizontal current speed at the sill in Sørfolda in March, April and May, positive is out of the fjord.

During March 1989 strong variability is evident in the upper 20 m, with several incidents of both outflow and inflow with speeds close to 0.2 m/s in both directions. The prevailing currents are directed out of the fjord below 20 m.

During April 1960 (Figure 5.11(c)) the currents have highest variability in the upper 15 m. The most frequent direction is outwards with speeds up to 0.3 m/s, interrupted by a strong inflow around 17^{th} April. In April 1989 (Figure 5.11(d)) the strongest variability is constricted within the upper 5 m. The most common direction is out of the fjord, with two short episodes of inflow.

Figures 5.11(e) and 5.11(f) display the currents during May 1960 and 1989. Both years show large variations within in the upper 5 m. The highest velocities are observed in the surface outflow in 1989, around 0.5 m/s, and intermittently disrupted by inflows. One significant incident of surface inflow is seen in May 1960, otherwise the currents are most often directed out of the fjord. Some periods of enhanced inflow is observed in the lower layers during 1989, mainly at 5-10 m depth.

5.6 Comparing vertical profiles between 1960 and 1989

Figure 5.12 shows monthly mean salinity profiles from Sørfolda and Nordfolda. The positions are shown in Figure 2.2 as red stars. The profiles are averaged over March, April and May for both 1960 and 1989. The same is done for the temperature, shown in Figure 5.13.

The salinity profiles from spring 1960 are seen as solid lines in figure 5.12. The surface salinity in Sørfolda decreases from March to April from about 33 to 23. Below 10 m only minor variations are apparent. The surface salinity in Nordfolda decreases as well, but not as much as in Sørfolda. In 1989 the difference between March and May is larger than observed in 1960. The reduction of surface salinity in Sørfolda is from 32 to 17. Comparing between the years, the stratification starts one month earlier in 1989 than in 1960. This means that the salinity profile in April 1989 matches the profile in May 1960. In Nordfolda the difference between 1960 and 1989 is even larger. Here the surface salinity in April 1989 is lower than the salinity in May 1960. The upper layer in Nordfolda is in general deeper than in Sørfolda.

The temperature profiles (Figure 5.13) have highest variability in the upper 50 m, both in Sørfolda and Nordfolda. All profiles are getting progressively warmer towards the end of spring. The variability between the years

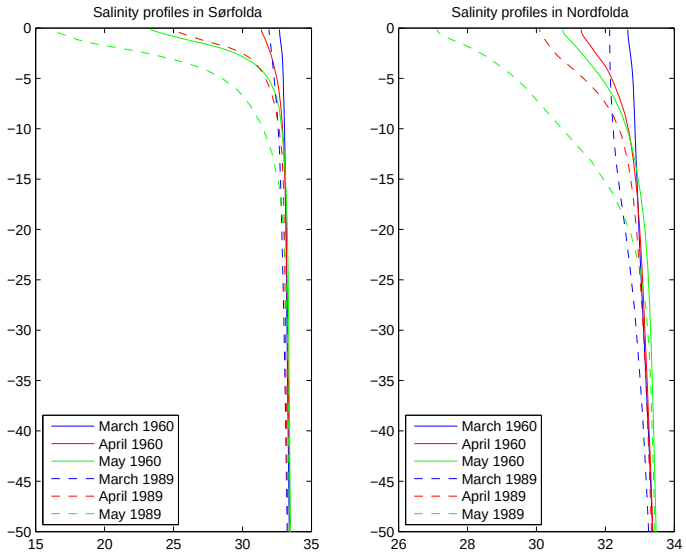

Figure 5.12: Monthly mean salinity in Sørfolda and Nordfolda, positions are shown as red stars in Figure 2.2.

is not as pronounced as seen in the salinity profile. The amplitude of the surface warming is slightly higher in 1960, starting off colder and ending up warmer than in 1989.

5.7 Circulation at the mouth of Leirfjorden

In Figure 5.14 the circulation pattern at the mouth of Leirfjorden is shown, this is at the inner end of Sørfolda. The Figures (a)-(e) all show the currents at 1 m depth from 17^{th} to 21^{st} April. This time period is chosen because of the normal estuarine circulation is reversed and then restored.

On 17^{th} April is the normal situation with outflow in Leirfjorden and Sørfolda. The current does not vary much across the fjord, except for boundary effects. On 18^{th} April the outflow is only present on the western side of Sørfolda, not in Leirfjorden. Entering 19^{th} April the current is directed into Sørfolda, strongest on the southern side. The current in Leirfjorden is also directed into the fjord following the topography. The next day the system is in between the two opposite circulation patterns, with an outflow in Leirfjorden and on the northern side of Sørfolda. On the southern side it is still inflowing water, all joining at the mouth of Leirfjorden. 21^{st} April the situation is getting close to the normal estuarine circulation with an outflow in the upper layer. But in the middle of Sørfolda the outflow meets the inflow

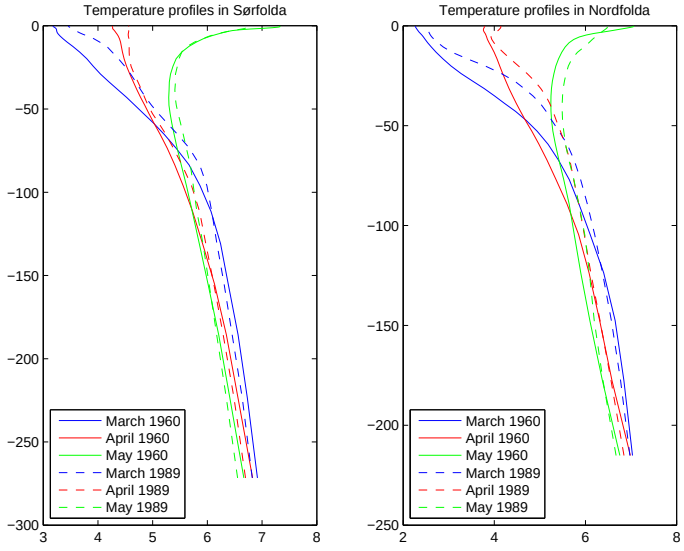

Figure 5.13: Monthly mean temperature in Sørfolda and Nordfolda, positions are shown as red starts in Figure 2.2.

and is pushed along the northern side.

Figure 5.15 shows the salinity distribution at the same time and place as the currents in Figure 5.14. On 17^{th} April there is a clear difference in salinity across the fjord, both in Leirfjorden and Sørfolda. This coincides with what is considered normal estuarine circulation. 18^{th} April show the same for Sørfolda, both no clear variance in Leirfjorden. Reaching 19^{th} April the cross fjord variance is missing and replaced with progressively decreasing salinity towards the head of the fjord. This is the same in Leirfjorden on 20^{th} April, but in Sørfolda a tongue of salt water is entering on the southern side. This is the same day as before, when the currents in Sørfolda were directed both into and out of the fjord. On 21^{st} April there is strong variability across Sørfolda when the normal estuarine circulation is setting up again. Inside Leirfjorden the salinity decrease towards the inner end, with no cross fjord variance.

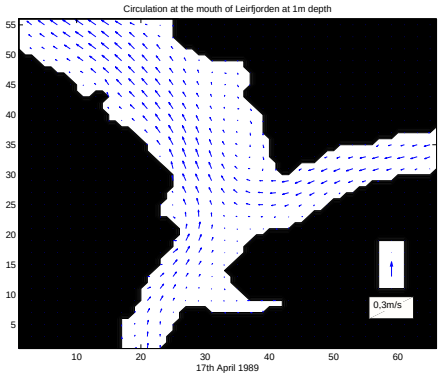

(a) 17^{th} April 1989

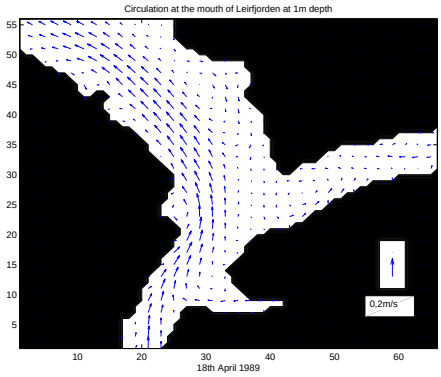

(b) 18^{th} April 1989

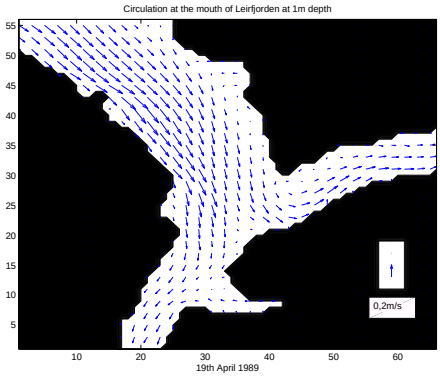

(c) 19^{th} April 1989

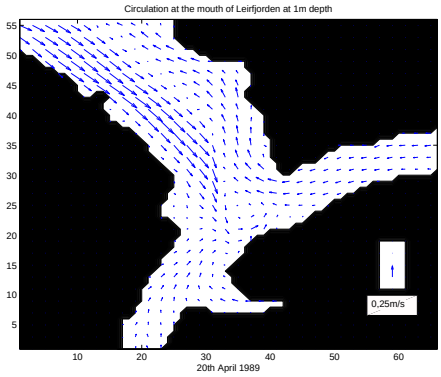

(d) 20^{th} April 1989

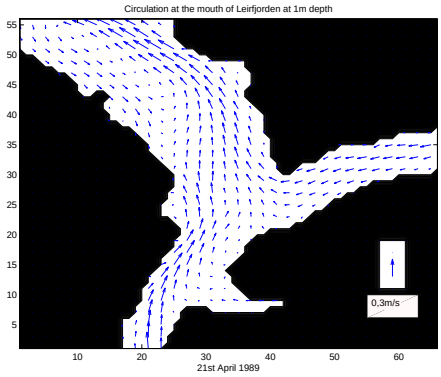

(e) 21^{st} April 1989

Figure 5.14: Circulation at the mouth of Leirfjorden at 1 m depth.

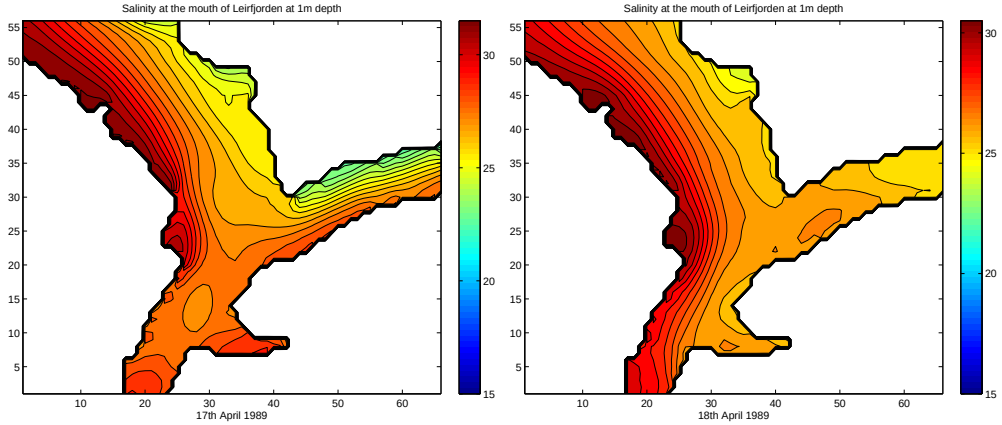

(a) 17^{th} April 1989

(b) 18^{th} April 1989

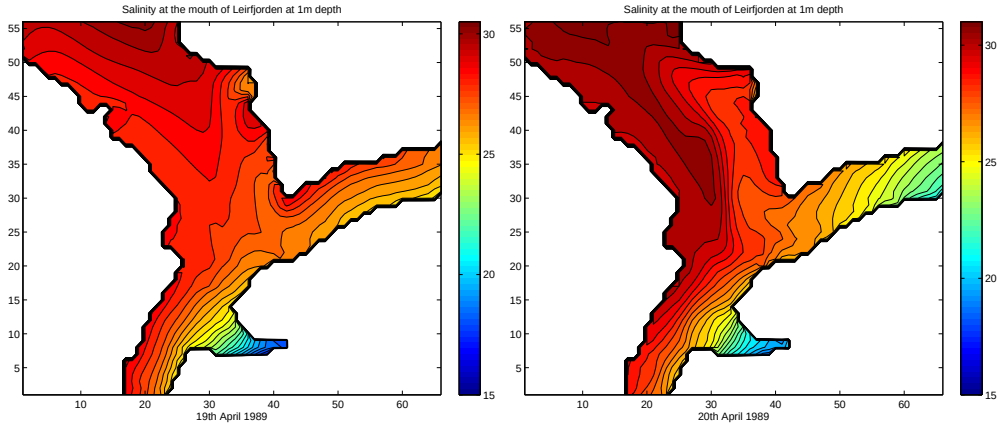

(c) 19^{th} April 1989

(d) 20^{th} April 1989

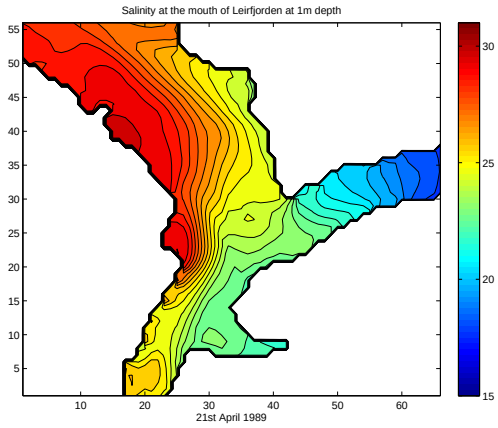

(e) 21^{st} April 1989

Figure 5.15: Salinity at the mouth of Leirfjorden at 1 m depth.

Chapter 6

Transport of eggs

The results from the particle tracking model are presented in this chapter. Data from the circulation model are used to transport the particles during the main spawning season in 1960 and 1989.

The first approach shows particles spreading at constant depths. Four different release times are used; 15^{th} March, 1^{st} April, 15^{th} April and 1^{st} May. The particles are advected for 21 days, being close to the incubation time for cod eggs. When the particles are held at fixed depths their movement support information about the overall transport in this depth. Especially the currents at 1 m depth are interesting because they illustrate the fate of pelagic eggs in the fjord system. Most mesopelagic eggs can be found in the whole water column down to 30 m depth with highest concentrations around 5-10 m, strongly varying with the vertical salinity structure.

The second approach uses a dynamical vertical egg distribution. This is a more realistic case that uses the neutral buoyancy distribution of Norwegian Coastal Cod (Figure 3.2). The same release times are used together with 21 days of advection.

6.1 Transport at fixed depths

From Figure 2.4(a) four release areas were selected; Sørfolda, Leirfjorden, Nordfolda and Vinkfjord. The particles were released with small spatial variations at 1 m, 10 m, 20 m and 30 m depth and was fixed to this depth. 324 particles was released at each spawning area, 1296 in total.

Figure 6.1 shows the trajectories for particles held constantly at 1 m depth. The release time was 15^{th} April and the particles were transported for 21 days in both 1960 and 1989. All particles released in Sørfolda 1960 are concentrated in the inner parts of the fjord. From Nordfolda and Vinkfjord

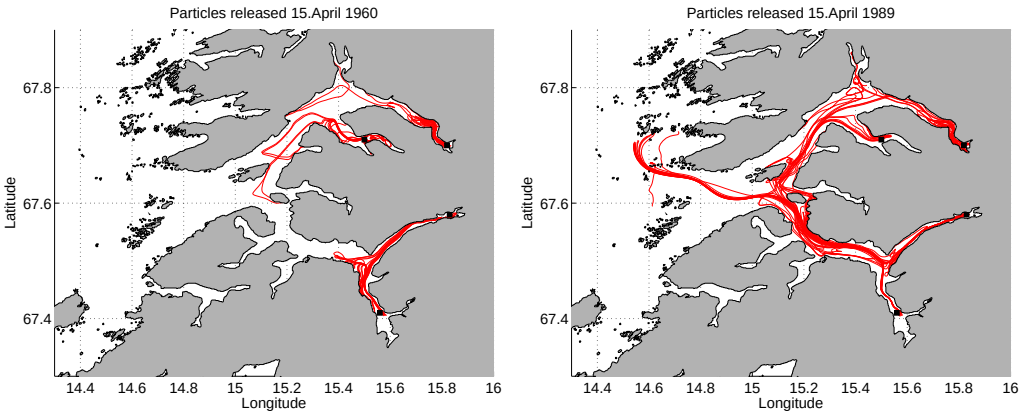

(a) 1960 at 1 m depth

(b) 1989 at 1 m depth

Figure 6.1: Particles released on 15^{th} April and transported for 21 days in 1960 and 1989, black boxes indicate release area.

some particles have left their spawning grounds, but none have left the fjord system. The particles released during 1989 show a larger spreading after 21 days. Most particles have left their origin, being transported either out of the fjord through the mouth or into another fjord branch.

Particles transported at 10 m and 20 m depth are shown in Figure 6.2. The spreading of particles at 30 m is not shown due to of strong similarity with 20 m. Figures 6.2(a) and 6.2(b) show the path of particles held at 10 m depth during 1960 and 1989, both released on 15^{th} April. Most particles stay within the fjord branch where they were released in 1960. In 1989 all particles released in Sørfolda, Leirfjorden and Nordfolda are retained close to release area. Only particles released in Vinkfjord spread out from their starting point, covering the outer part of Nordfolda.

The spreading of particles at 20 m depth is similar to 10 m (Figures 6.2(c) and 6.2(d)). The degree of retention is large for particles released in Sørfolda, Leirfjorden and Nordfolda. A small number of particles from Vinkfjord leave the fjord in 1960, compared to a larger number in 1989. The particles at 20 m depth are spreading out towards the mouth area in 1989, in contrast to the particles in 10 m depth that stay within Nordfolda.

Table 6.1 shows the percentage of particles that ends up outside the fjord system after being transported around for 21 days. The dates are different release times, the same for both years. In total only a few particles are advected out of the fjord in 1960. This occurs with the release time of 1^{st} May. In 1989 the total number of particles leaving the system is larger.

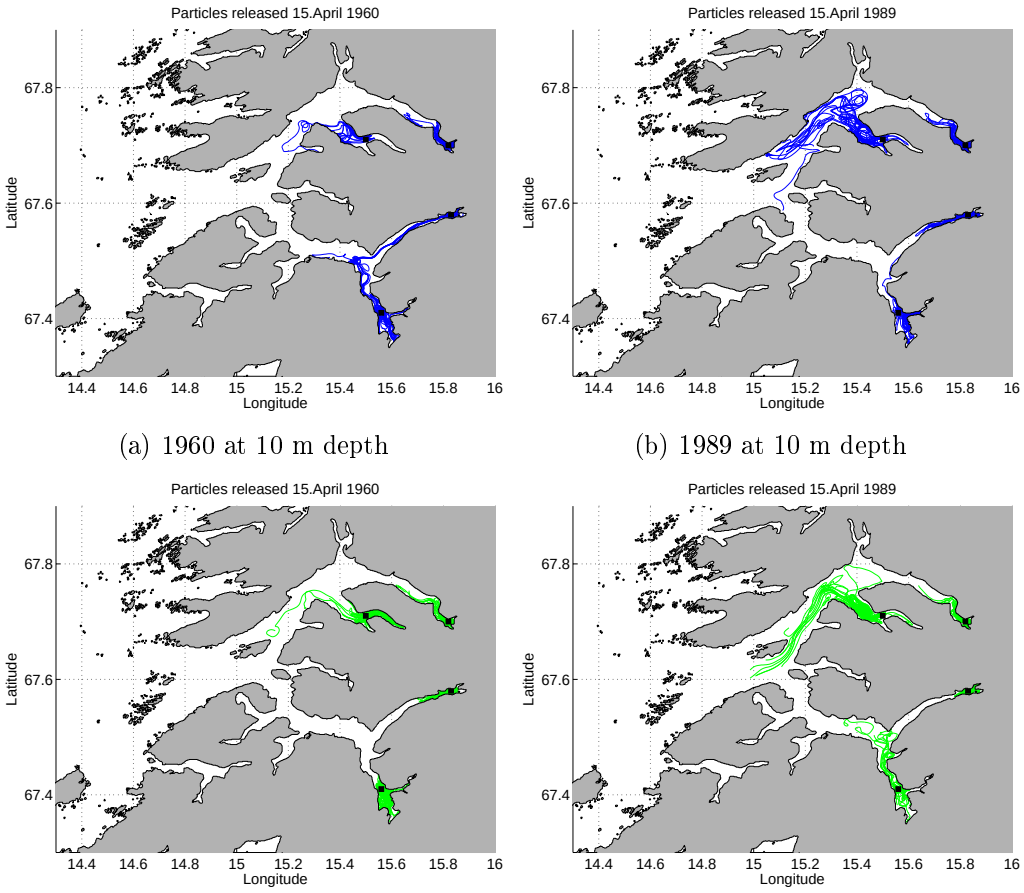

(a) 1960 at 10 m depth

(b) 1989 at 10 m depth

(c) 1960 at 20 m depth

(d) 1989 at 20 m depth

Figure 6.2: Particles released on 15^{th} April and transported for 21 days in 1960 and 1989, black boxes indicate release area.

Especially at 1 m depth there is a great number of particles spreading out of the fjord on 15^{th} March and 15^{th} April.

After the particles have been drifting for 21 days, the total distance travelled was calculated by using the offset between the first and the last position. When the total distance travelled is less than 25 km, the particle is considered retained inside the same fjord where it was released. If the total distance is more than 25 km, the particle has either left the whole fjord system or has entered another fjord branch. This specific distance is used since it is about half the length of the fjord. Table 6.2 shows the percentage of particles remaining within a radius of 25 km from spawning area.

In 1960 the percentage of particles being trapped close to the spawning

Table 6.1: Percentage of particles leaving the fjord system.

		15thMarch	**1stApril**	**15thApril**	**1stMay**
1960	1 m	0	0	0	3,4
	10 m	0,3	0,9	1,5	0
	20 m	0	0	0	0
	30 m	0	0	0	0
1989	1 m	10,5	1,9	23,8	0
	10 m	1,9	5,6	0,3	0
	20 m	0	0,3	0	4,3
	30 m	0	0	0	0,6

ground is higher than 83% at all depths at all times. 1^{st} April is the time of largest spreading of particles. The Table 6.1 showed earlier that no particles from 1^{st} April 1960 left the fjord system, which means that all 17% that travelled more than 25 km are still within the fjord system. The degree of

Table 6.2: Percentage of particles remaining within a radius of 25 km from spawning area.

		15thMarch	**1stApril**	**15thApril**	**1stMay**
1960	1 m	98,8	83,0	96,0	87,4
	10 m	99,1	96,3	97,8	99,1
	20 m	100	100	100	100
	30 m	100	100	100	100
1989	1 m	71,3	84,3	51,5	71,9
	10 m	96,9	79,9	98,2	100
	20 m	100	99,7	99,4	93,5
	30 m	100	100	100	99,4

retention in 1989 is in general lower than in 1960, except for 1^{st} April of 1 m depth. The percentage of particles at 1 m depth staying close to release point varies between 52% and 84%. The dispersion of particles is most pronounced on 15^{th} April 1989. About half the total number of particles have disappeared from their spawning grounds. When comparing with Table 6.1 it can be seen that not all particles travelling far away have left the fjord system, many have also covered a large distance within the fjord.

6.2 Dynamical vertical distribution

For a more realistic transport of eggs, the particles used in section 6.1 are added the possibility of vertical displacement, resulting in a dynamical vertical distribution. Each particle obtains a specific level of neutral buoyancy according to the distribution in Figure 6.3. For easier interpretation of the results, the eggs are divided into five buoyancy groups, which will be used later in evaluation of the results.

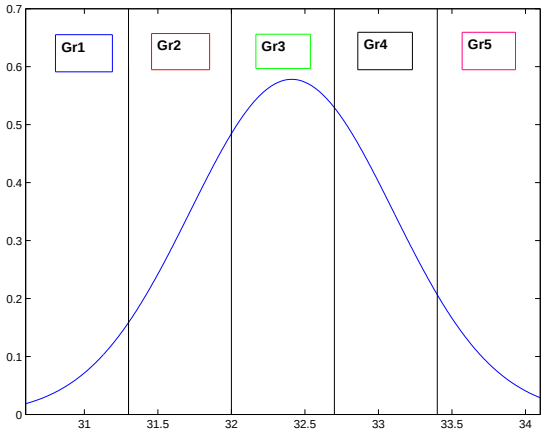

(Stenevik *et al.*, 2008)

Figure 6.3: Neutral buoyancy of Norwegian Coastal Cod, divided into five buoyancy groups for easier comparison of results.

In every setup approximately 15000 eggs are used with a diameter of 1.4 mm. All are released at 20 m depth and equally distributed at the four spawning grounds; Sørfolda, Leirfjorden, Nordfolda and Vinkfjord. The particle tracking model calculates the vertical velocity depending on the density difference between the eggs and the surrounding water, using equation 3.3. Then the vertical movement is computed based on the vertical velocity and the eddy diffusivity coefficient, with an internal timestep of 6 s. The density structure, the eddy diffusivity coefficient and the current speed are imported from the circulation model, and updated every hour. The output from the particle tracking model is stored every hour. The simulations are continued for 21 days, being close to the incubation time for cod eggs.

Trajectories from a selection of eggs in buoyancy group 1 and 2 are shown in Figure 6.4. The figure shows the path covered during 21 days by the particles for the years 1960 and 1989, with the same release time 15^{th} April.

Figures 6.4(a) and 6.4(b) show transport of eggs in buoyancy group 1 for 1960 and 1989. In 1960 there are a significant number of eggs being

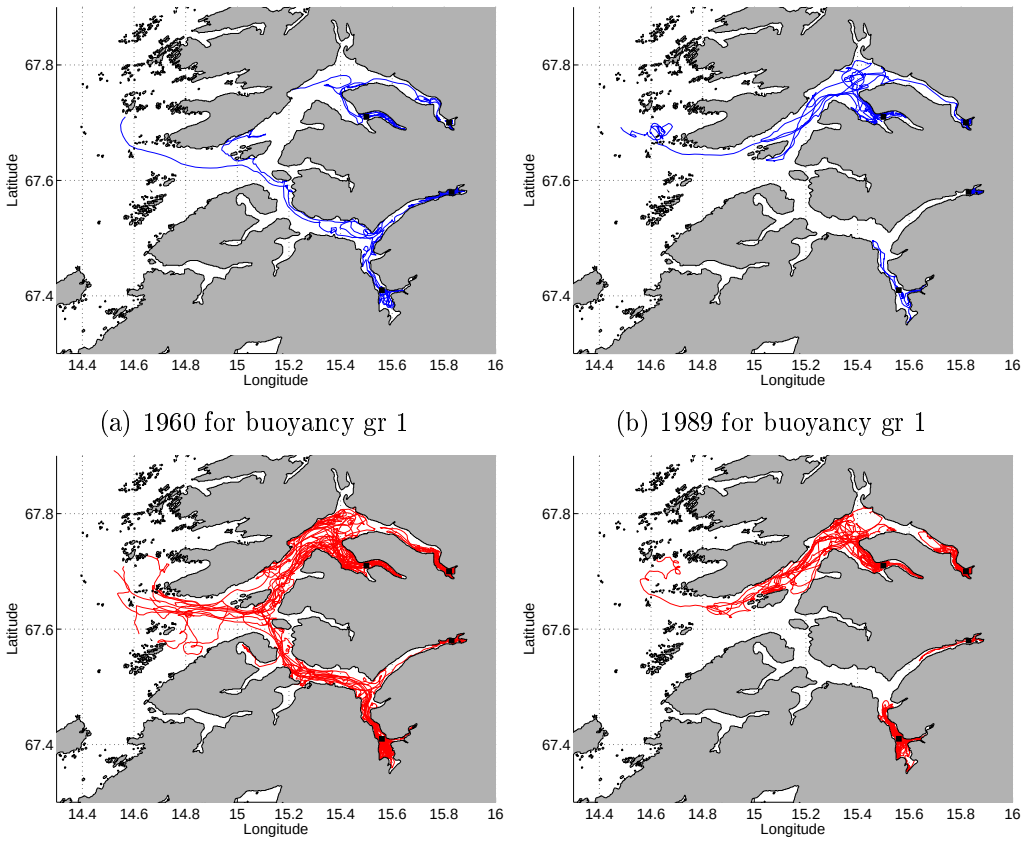

(a) 1960 for buoyancy gr 1

(b) 1989 for buoyancy gr 1

(c) 1960 for buoyancy gr 2

(d) 1989 for buoyancy gr 2

Figure 6.4: Trajectories from eggs released on 15^{th} April and transported for 21 days in 1960 and 1989, black boxes indicate spawning grounds.

transported away from their spawning grounds. From Sørfolda, Leirfjorden and Vinkfjord the eggs are spreading out in the fjord system. No eggs from Nordfolda have left their origin, only eggs from Vinkfjord have been advected into Nordfolda. In 1989 the spreading of eggs away from the spawning areas is different. Here all eggs from Sørfolda and Leirfjorden have been trapped in their respective fjord branch. But the trajectories leaving Vinkfjord show stronger spreading inside Nordfolda and also leaving the fjord system. Eggs being spawned in Nordfolda are both being retained and spread out.

The spreading of eggs in buoyancy group 2 are shown in Figures 6.4(c) and 6.4(d). The trajectories from 1960 covers the whole fjord system. All spawn-

ing grounds show a large dispersal of eggs, both within the fjord branches and out through the mouth. In 1989 only eggs from Vinkfjord show large dispersion, all other spawning areas have a stronger degree of retention.

Figure 6.5 shows transport of eggs in buoyancy group 3 and 4. Buoyancy group 5 is not shown since it is almost identical to buoyancy group 4.

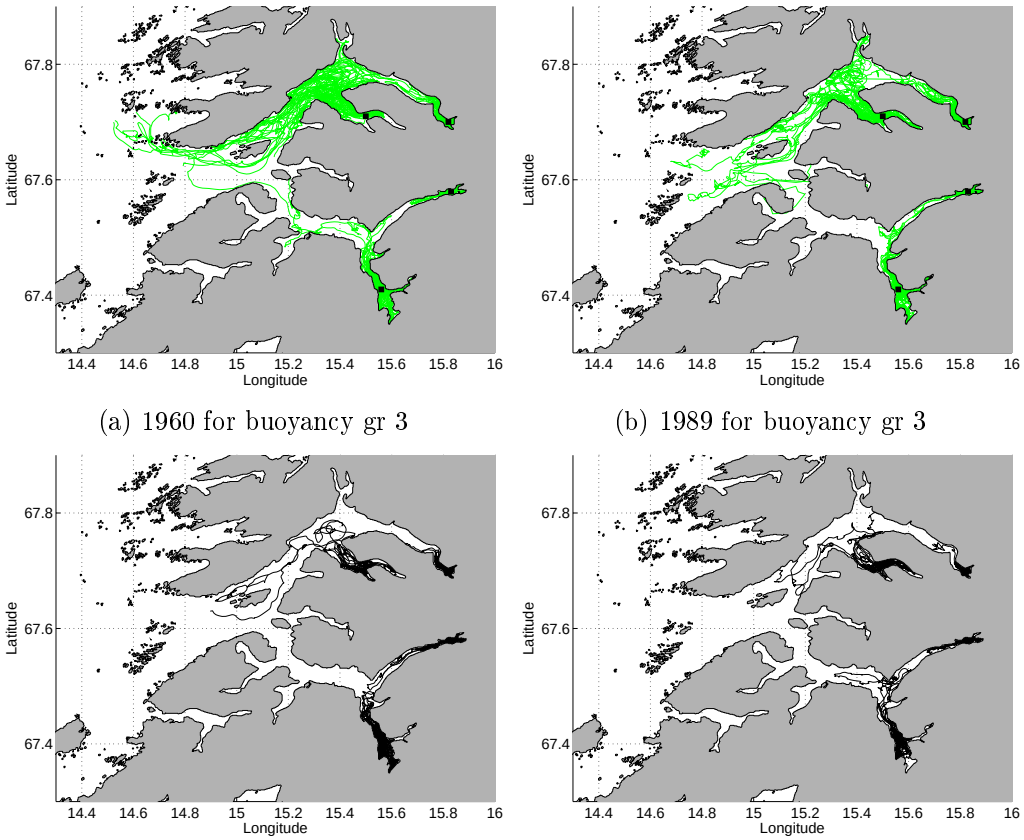

(a) 1960 for buoyancy gr 3

(b) 1989 for buoyancy gr 3

(c) 1960 for buoyancy gr 4

(d) 1989 for buoyancy gr 4

Figure 6.5: Trajectories from eggs released on 15^{th} April and transported for 21 days in 1960 and 1989, black boxes indicate spawning grounds.

Figures 6.5(a) and 6.5(b) show the paths covered by buoyancy group 3. The eggs spawned in 1960 have been subjected to large spreading. Especially in Nordfolda eggs are located in the whole fjord. The majority of eggs being spread out are coming from Vinkfjord, some are also leaving the fjord system. From Sørfolda a small portion of eggs are located in main part of the fjord. All eggs released in Leirfjorden are retained there. 1989 show less dispersal of eggs in the whole fjord system. Eggs from Vinkfjord are transported out

into Nordfolda and towards the mouth area. Most particles from Nordfolda, Sørfolda and Leirfjorden remain close to their origin.

Transportation of eggs in buoyancy group 4 are shown in Figures 6.5(c) and 6.5(d). These trajectories are more concentrated than the ones for buoyancy group 3. The main part of eggs spawned in Sørfolda, Leirfjorden and Nordfolda are being retained close to their spawning grounds. In Vinkfjord some eggs are trapped inside the fjord and some are transported out to Nordfolda. Comparison between 1960 and 1989 shows only minor differences.

When modeled vertical distribution is included, the total number of particles leaving the fjord system is different than for transport at fixed depths. In Table 6.3 the number of eggs ending up outside the fjord system is calculated. For 1960 the percent is largest for the lightest buoyancy group, and increasing with time. For the other buoyancy groups the number of eggs lost is smaller. In 1989 mainly eggs in buoyancy group 1 and 2 are transported out of the region, this occurs on 15^{th} March and 1^{st} April. From 15^{th} April and forwards the percentage of eggs leaving the fjord system is small in all buoyancy groups. The major difference between 1960 and 1989 is in buoyancy group 1 (the lightest one). This group has largest dispersion late in spring in 1960 and early in 1989.

Table 6.3: Percentage of eggs that have left the fjord system.

		15thMarch	**1stApril**	**15thApril**	**1stMay**
1960	gr 1	0	3,4	11,5	13,6
	gr 2	0,3	4,2	9,8	3,0
	gr 3	0,7	4,1	6,4	0,3
	gr 4	0,6	0,8	1,8	0
	gr 5	0	0,1	0	0
1989	gr 1	10,0	13,9	1,2	1,8
	gr 2	5,7	13,0	2,2	1,2
	gr 3	2,2	7,6	1,2	0,9
	gr 4	0,1	0	0	0,1
	gr 5	0	0	0	0

In Table 6.4 the percentage of eggs staying within a radius of 25 km after 21 days is shown. Since 25 km is approximately half the length of both Sørfolda and Nordfolda, the eggs are considered trapped close to spawning site when remaining inside this radius.

In 1960 the percentage of retention is highest in the beginning of spring (15^{th} March). Later the retention is decreasing, especially for buoyancy group 1 (the lightest). For all the other groups the proportion that stay close to

Table 6.4: Percentage of eggs staying within a radius of 25 km from the spawning site.

		15^{th}March	1^{st}April	15^{th}April	1^{st}May
1960	gr 1	93,4	81,8	78,0	79,7
	gr 2	93,3	80,1	83,8	95,2
	gr 3	93,9	86,1	90,3	99,3
	gr 4	96,6	96,3	97,9	100
	gr 5	98,3	99,8	99,9	100
1989	gr 1	73,8	81,5	98,0	96,2
	gr 2	84,0	80,4	96,7	96,4
	gr 3	95,1	89,6	97,7	97,4
	gr 4	99,8	99,9	99,9	99,7
	gr 5	99,4	99,7	99,9	100

spawning area is high at all times. The lowest percentage of eggs staying close to spawning grounds occurs on 15^{th} April in buoyancy group 1 (78%). 1989 shows an opposite pattern. The degree of retention is smallest in the beginning (73,8%) and increasing towards 15^{th} April, most pronounced for group 1. For 15^{th} April and 1^{st} May the amount of leakage is very small for all buoyancy groups.

Mean distance travelled from spawning grounds by each buoyancy group is displayed in Figure 6.6, from 15^{th} April and 21 days ahead. In 1960 all

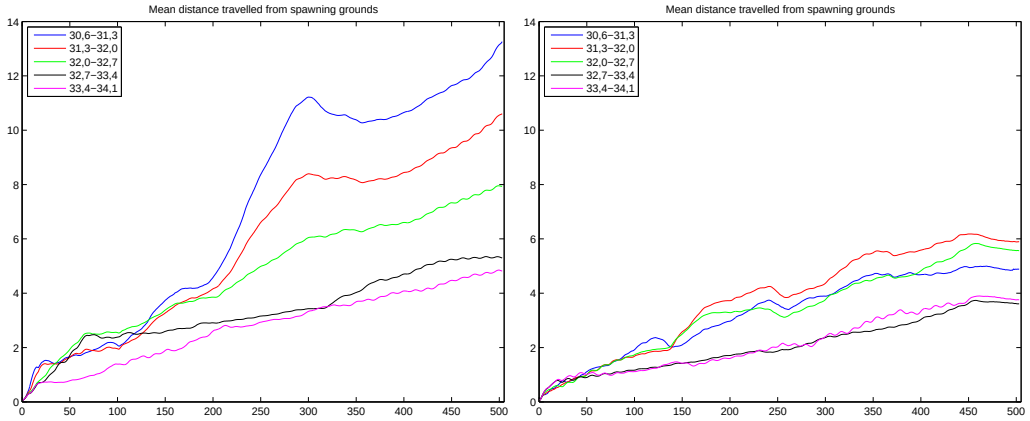

(a) 1960 (b) 1989

Figure 6.6: Mean distance [km] versus time [hours] travelled from spawning grounds, released 15^{th} April and 21 days ahead.

buoyancy groups keep close together in the beginning of the simulation. After approximately 10 days the paths separate, with the lightest buoyancy groups travelling the longest distance. The separation coincides with an incident of low salinity in the surface layer and enhanced outflow at the end of April, see Figure 5.10 and 5.11. After 21 days, the mean distance varies between 5 km and 13 km, from heavy to lighter buoyancy groups. During the simulation for 1989 all curves stay closer together for the whole run. The two heaviest buoyancy groups remain within 4 km after 21 days, the others do not exceed more than 6 km from the spawning ground. The major difference between 1960 and 1989 is found in the three lightest groups, where they travel about twice as long in 1960 compared to 1989.

6.3 Difference between spawning grounds

Figure 6.7 shows the mean distance travelled by eggs with a dynamical vertical distribution for 21 days. The different curves are functions of the four different spawning sites; Sørfolda, Leirfjorden, Nordfolda and Vinkfjord. Both years show that eggs released in Vinkfjord travel much further away from spawning area than at the other sites. All eggs travel a shorter distance in 1989 compared to 1960.

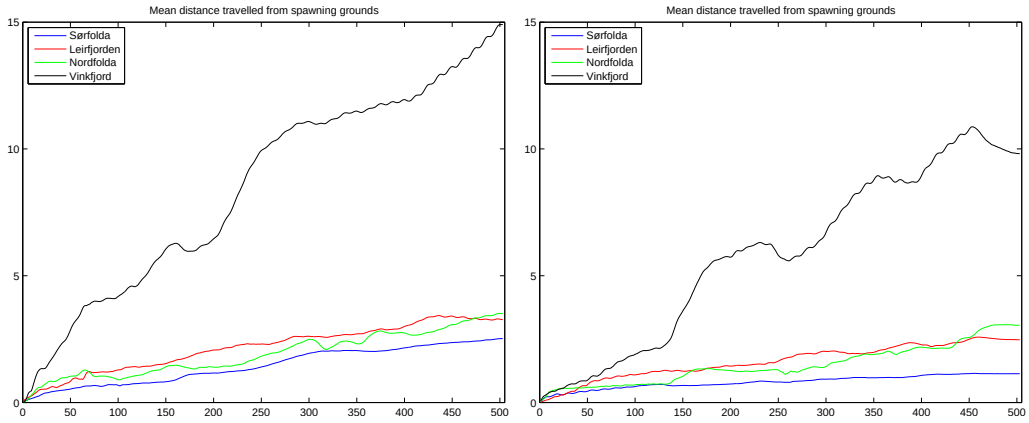

(a) 1960 (b) 1989

Figure 6.7: Mean distance [km] versus time [hours] travelled from spawning grounds, released 15^{th} April and 21 days ahead.

Chapter 7

Discussion

7.1 Model performance

The Regional Ocean Modeling System (ROMS) uses the primitive equations on a finite grid. With a horizontal resolution of 200 m and 35 vertical sigma layers the coverage is rather good. However, all variations on sub-grid scale has to be parameterized, causing restrictions on the model performance. A limitation of this model setup is the maximum bottom depth of 300 m. The bathymetry of the fjord system shows large areas of depth down to approximately 500 m. This was done due to stability problems with the model run. The main results of this is missing representation of the bottom layers. For the purpose of this work, where transport of pelagic and mesopelagic eggs confined to the upper 50-70 m is the main objective, this limitation is acceptable. However, the model setup can not be used to study renewals of bottom waters.

7.1.1 Wind forcing

The atmospheric forcing used in these simulations is derived from the ERA-40 reanalysis from 1957 to 2002, with a horizontal resolution of 1 degree. This means that the resolution is coarse in relation to small-scale modeling. For most of the variables, (cloud cover, air pressure, specific humidity, precipitation and air temperature), the offset is not too large, but regarding the wind data the errors might be substantial. The wind field used in the simulations (Figure 7.1) do not have any horizontal variations within the model area. This is in large contrast to most observations in fjords where the winds are known to have large spatial variations both in strength and direction. Steep mountains surrounding fjords cause channeling of winds, often directed either into or out of the fjord. Svendsen and Thompson (1978) concluded that the

wind stress is the most important forcing for the circulation in a fjord. Considerable runoff causing strong stratification traps the wind-stress response to the surface layer.

Figure 7.1 shows the wind used in the simulations. The upper panel shows the period from 1^{st} March to 31^{st} May in 1960, and the lower panel covers the same time period during 1989. The wind varies substantially both in strength

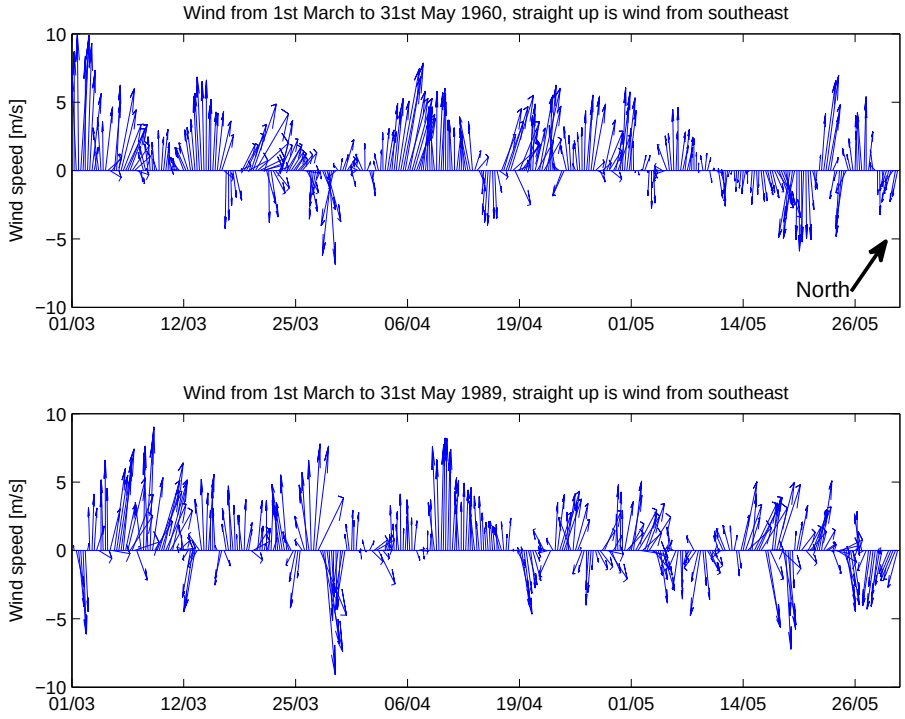

Figure 7.1: The wind forcing from ERA-40 relative to model grid, rotated 45° in clockwise direction relative to latitude.

and direction during this period in both 1960 and 1989. The wind speed never exceeds 10 m/s and the most dominant wind directions are from south-east and north-east (see Figures 7.2(a) and 7.2(b)). No obvious differences are observed between the years, except for a stronger north-westerly component in 1960 towards the end of the time period.

To compare the wind used in the simulations with observations, data from Skrova in Vestfjorden are used (see Figure 2.1). Figure 7.2 shows the most frequent wind directions from the ERA-40 wind forcing (upper panel) together with measurements at Skrova (lower panel), during spring 1960 and 1989. The most frequent wind directions at Skrova are easterlies and south-westerlies, as was shown by Sundby (1982). The south-westerly winds have

a stronger southerly component in 1960 compared to 1989. Easterly winds

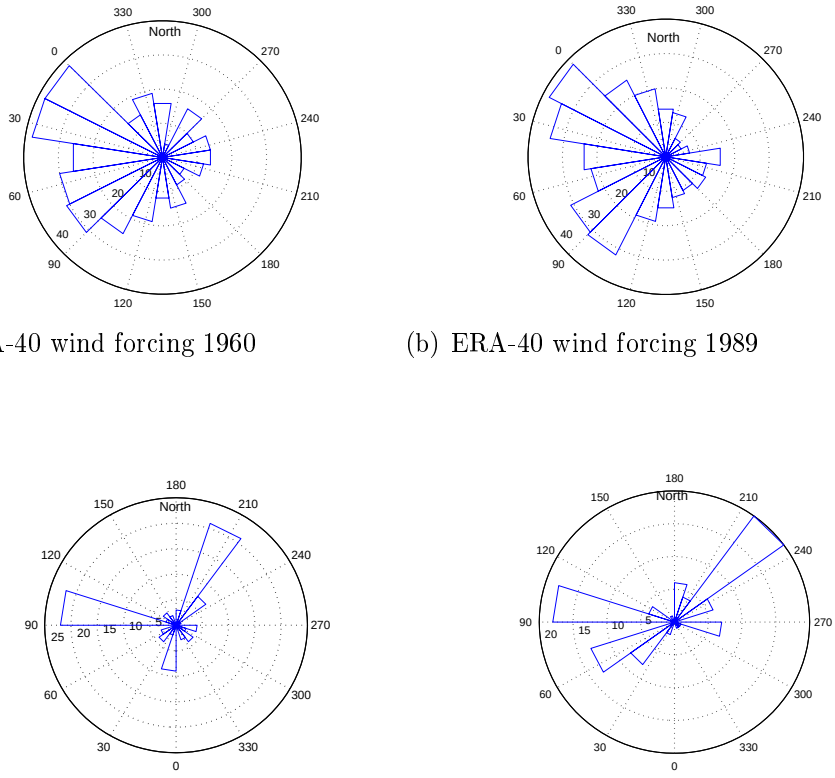

(a) ERA-40 wind forcing 1960

(b) ERA-40 wind forcing 1989

(c) Observations at Skrova 1960

(d) Observations at Skrova 1989

Figure 7.2: Histogram of wind directions from the ERA-40 wind forcing (upper) and observations at Skrova in Vestfjorden (lower) during March, April and May 1960 and 1989.

in Folda are directed out of the fjord in the mouth area and in most fjord branches. This case is assumed to enhance the estuarine circulation and cause strong mixing in the surface layer. Strong mixing results in deepening of the brackish layer and increased surface salinities. The other event with south-westerly winds might cause a more complicated situation. These winds are directed into Nordfolda and Leirfjorden, and are likely to increase the transport from Sørfolda to Nordfolda. The south-westerly winds are strong and will cause heavy mixing. In some fjord branches a reduced or even reversed estuarine circulation can be expected during these incidents.

The winds used in the simulations and the observations at Skrova are

clearly different, both in wind speed and direction. Especially the strong south-westerly winds seen in the observations are lacking in the wind forcing from ERA-40. The observations also show a distinct easterly component, compared to the model winds that varies between north-easterly and south-easterly. The wind speed is general higher in the observations than in the forcing.

These differences in model wind and observations will cause an underestimate of wind energy input to the model simulations. Reduced energy input to the system results in weaker surface currents and less energy available for mixing. In a fjord system with estuarine circulation, reduced mixing will generate a thinner surface layer with lower salinity than what would be observed. The error in wind direction might have an impact on events of reduced and reversed estuarine circulation. The observations from Skrova show that the wind directions alternates between two situations, but the model wind is dominated by one direction. Inflow at the sill in Sørfolda, (Figure 5.11), is highly correlated with the north-westerly wind events, (Figure 7.1). On average the model shows two incidents of reversed estuarine circulation per month, (Figure 5.11). With stronger variability in wind direction this number is expected to be higher.

Stronger variability in wind direction and strength could affect the dispersal of eggs. One reason is the increased interaction with the shelf areas through larger number of reversals. An incident of reversed estuarine circulation could cause eggs at lower levels to be transported out of the fjord. Stronger wind energy input will increase the salinity in the surface layer. Then a larger portion of the eggs have neutral buoyancy similar to the mixed layer, and hence larger possibility for eggs to be situated in the strong surface outflow. It is likely that more accurate wind forcing could increase the spreading of eggs in the fjord system.

Non-local wind effects

Northerly winds along the Norwegian coast will cause a surface volume transport away from the coast, giving rise to upwelling at the coast. In the opposite case southerly winds will cause downwelling at the coast. The two main wind directions in Vestfjorden, easterly and south-westerly, will generate upwelling and downwelling at the coast just outside Folda (Furnes & Sundby, 1981). An upwelling event will increase the outward transport in the upper layers in a fjord, a downwelling event will transport the upper layer into the fjord (Asplin *et al.*, 1999). These processes are rapid and $\sim$50% of the upper water layer may be replaced within 1-2 days, which will have a large impact on the local environment. Southerly winds will transport planktonic organisms into

the fjord, and northerly winds can increase the offshore transport of early life stages of local fish populations. Due to small geographic model area and low-resolution wind data these processes are not resolved in the model. The outcome will be reduced interaction between the coastal and fjord waters.

7.1.2 Hydrography and circulation

The results in chapter 5 show that the model recreate the main features related to the estuarine circulation. The salinity is lowest at the inner ends of the fjord branches, and increasing towards the mouth. Figure 5.6 displays the strong outflow in the surface layer and weaker inflow below, corresponding to the estuarine circulation. This figure also shows the variation of surface layer thickness across the fjord, verifying the influence of rotation. Rotation causes motion to be deflected towards right. This results in outflowing currents to be deflected towards east in Sørfolda.

Currents in coastal areas and fjords have strong temporal variations, as illustrated in Figure 5.11. The surface current is highly depending on fresh water flux and wind forcing. If the fresh water influence is large and stratification strong, the wind influence is limited to the brackish layer. The strong variations in inflow and outflow, especially in the surface layer, recreated by the model seems to be realistic. The periodically strong outflow is a result of the changing river input. Together with this the varying wind cause the fluctuations between outflow and inflow. As discussed earlier the wind input is not expected to be representative for the area, however, the oscillation in strength and direction are quite realistic. Hence, the time of reversal might not be correct, but the number and strength may be quite close.

When comparing the model results from 1960 and 1989, distinct differences can be observed. The salinity in 1960 is in general higher than in 1989. The major difference in forcing for the two model runs is the fresh water discharge. All results verify that the difference in fresh water volume flux has a large impact on the estuarine circulation. This means that the surface current is frequently stronger in 1989 than in 1960, see Figure 5.8. The compensating current below the surface layer is also observed, but the location and strength is more variable. The salinity profile in Figure 5.12 illustrates the great difference in fresh water content between 1960 and 1989. This confirmes that interannual variations in fresh water discharge have a large impact on salinity structure and circulation.

Rotation

The influence of rotation was discussed in section 3.1.1. Here this theory will be used together with the data displayed in Figure 5.12 to calculate the internal Rossby radius. The salinities and depth of the upper layer are then a calculated mean from April 1960 and 1989. Equation (3.1) is used with latitude 67.5°N:
April 1960:

$$S_1 = 32, \rho_1 = 1025.35, S_2 = 34, \rho_2 = 1026.94, T = 4.5, h_1 = 10m$$

$$R = 2.9km$$

April 1989:

$$S_1 = 28, \rho_1 = 1022.18, S_2 = 34, \rho_2 = 1026.94, T = 4.5, h_1 = 7m$$

$$R = 5.0km$$

These calculations show that the internal Rossby radius is larger in 1989 than in 1960 during the same period. The difference is caused by a fresher surface layer in 1989, hence a stronger stratification. Considering the width of the fjords, (Sørfolda - 3.0 km, Leirfjorden - 1.6 km, Nordfolda - 4.0 km), this difference in internal Rossby radius is significant. Rotation is not considered to be important in neither of the two years in Leirfjorden. During April 1960 the internal Rossby radius is comparable or smaller than the width of Sørfolda and Nordfolda, which means rotation is important. During 1989 the internal Rossby radius is longer than the widths of both the two main fjords, hence rotation is less important. This illustrates the importance of changing stratification on rotational effects. These two examples are from the same period in two different years, but the change in internal Rossby radius can also occur in a transition period during one season.

7.2 Transport of eggs

The results generated by the circulation model are used to simulate the transport of eggs in the fjord system using a particle tracking model.

7.2.1 At fixed depths

The first attempt describes advection of particles at fixed depths. For 21 days the particles are held at the depth of 1 m, 10 m, 20 m and 30 m. This approach is independent on vertical density structure and mixing, and

support information about the overall transport at constant depths. Findings from these simulations are found in section 6.1. These results are used to illustrate the fate of particles held at 1 m depth through the run in 1960 and 1989, see Figure 7.3. The blue columns are portion of particles being trapped close to spawning grounds, the green columns are particles being transported within the fjord system and red columns are the percentage of particles leaving the fjord. As commented before, particles staying at 1 m depth have the smallest degree of retention. Almost all the other particles are trapped close to the release area. Comparing 1960 and 1989, the percentage of particles staying close to spawning grounds is largest in 1960. There is a greater portion both leaving the fjord and being transported within the fjord system in 1989. These results correlate to the fact that the surface

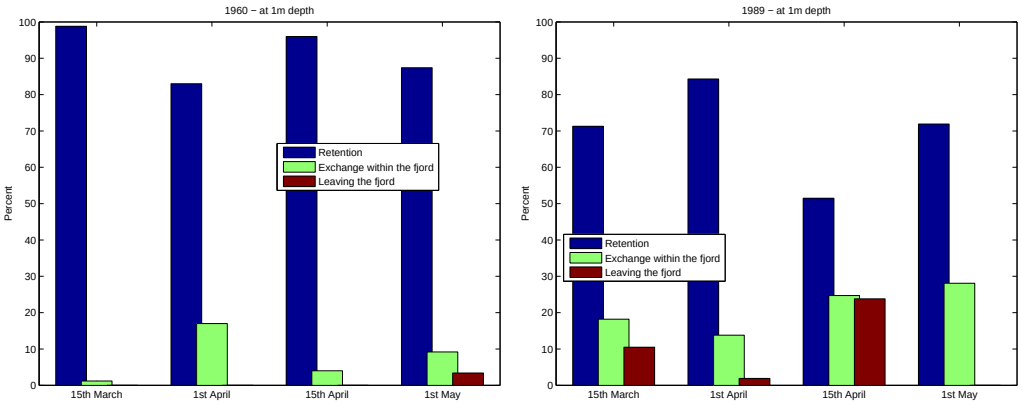

(a) 1960 (b) 1989

Figure 7.3: Overview of particles held at 1 m depth.

currents were stronger in 1989 compared to 1960, which would be expected to cause more spreading of particles confined to the surface layer. In the lower layers the difference was not that obvious, neither in currents nor spreading of particles.

Assuming these particles are cod eggs, almost all eggs spawned in 1960 would stay inside Sørfolda and Nordfolda. However, in 1989 eggs drifting at 1 m depth have a large probability of being transported away from their spawning area. Especially in late spring (from 15^{th} April and 1^{st} May) the possibility of being advected far away is quite large. Hence, the vertical position of eggs are important and has a large impact on their paths.

7.2.2 With dynamical vertical distribution

To make the particles behave more like cod eggs, the possibility of vertical displacement is included, resulting in a dynamical vertical distribution. Each egg is assigned a neutral buoyancy and a vertical velocity is calculated, according to the theory in section 3.2. The ascending or descending velocity is depending on the density structure surrounding the egg, provided by the circulation model. The vertical mixing is accounted for when computing the actual vertical distribution of the eggs. Including all these variables, the vertical distribution is calculated for eggs with neutral buoyancy according to CC. The results from these considerations are shown in section 6.2, where the buoyancy distribution is divided into groups according to the Figure 6.3.

The results are used in Figure 7.4, showing what happens to the eggs in buoyancy group 1 (the lightest) after being advected for 21 days. This group is chosen because of having the largest amplitude when comparing between the years and with different spawning time. The other groups show the same pattern, but with reduced variability for the heavier egg groups. The blue columns are percentage of eggs being retained close to spawning area, the green columns show exchange within the fjord system and the red columns are eggs transported out of the fjord. As commented earlier the degree of

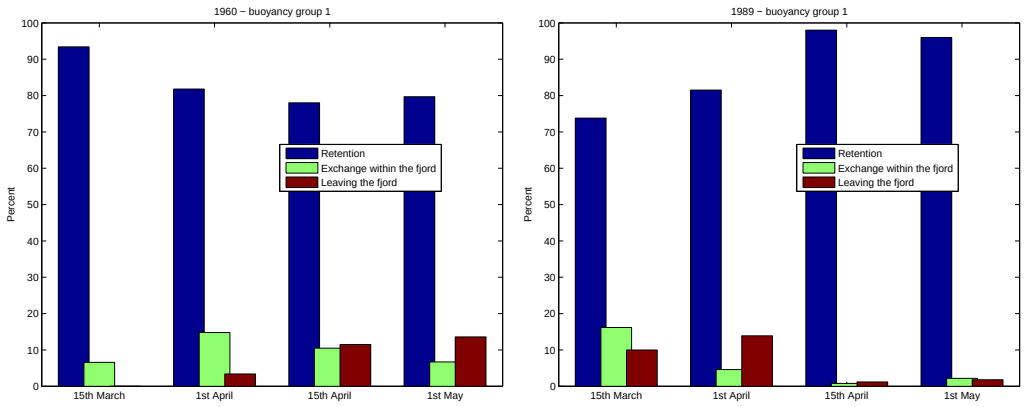

(a) 1960 (b) 1989

Figure 7.4: Overview of eggs from buoyancy group 1.

retention in 1960 is decreasing with increasing spawning time. The number of eggs being trapped is increasing with increasing spawning time in 1989. Towards the end of spring 1989 only a few eggs are spreading away from their origin.

The development in 1960 might be due to later onset of the estuarine

circulation. Early in spring several eggs stay inside the fjord because the outgoing current is weak. Figure 5.10 shows that stratification in Sørfolda is weak until the end of April, before it is getting stronger during May. When the surface current is getting stronger the spreading of eggs also increases in late April and May. However, since the fresh water input in 1960 is not very strong, the surface salinity does not decrease much. Which in turn means that the lightest eggs are floating in the upper water column and getting transported further away than the other eggs.

1989 shows a different pattern than 1960. The strong stratification in early April might explain some of the development, see Figure 5.10. A fresh surface layer this early means that the estuarine circulation has already started. Then an outwards flow in the upper layer cause the eggs spawned on 15^{th} March and 1^{st} April to spread away from their starting point. However, later in spring the surface salinity is getting progressively lower, see Figure 5.10. At this point the eggs are heavier than the surrounding water and sink below the fresh surface layer. By doing this the eggs are avoiding the strong surface current directed out of the fjord, and are getting retained at their spawning ground.

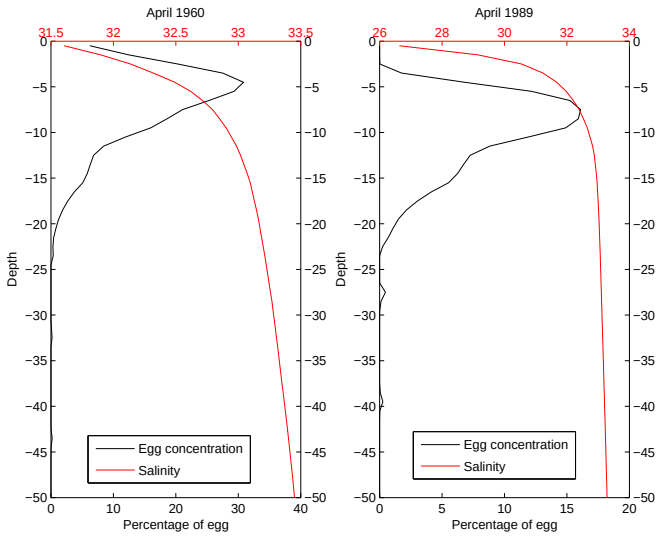

Figure 7.5: The vertical distribution of eggs according to the local salinity profile from April 1960 (left) and 1989 (right), at a station in Sørfolda (Figure 2.2).

Figure 7.5 illustrates the vertical profile of Norwegian Coastal Cod eggs according to the corresponding salinity profile for April 1960 and 1989. The

salinity profile is a monthly mean for April, as seen in Figure 5.12, and the eggs have the buoyancy distribution as shown in Figure 6.3. The concentration of eggs is a function of the density difference and the eddy diffusion coefficient (Ådlandsvik, 2000).

The major difference between 1960 and 1989 is the surface salinity, being close to 31.8 in 1960 and 26.6 in 1989. With this difference in salinity the concentration of eggs near the surface has changed. In 1960 some eggs are situated close to the surface and the maximum is around 5 m depth. However, in 1989 the eggs are all positioned below 2.5 m, with highest concentration around 7.5 m depth. When the surface layer is thin, as in 1989, this difference in vertical distribution is important. When the eggs are at a lower level in the water column, the possibility of being transported away is much smaller and the degree of retention is larger.

The same vertical profile of eggs is shown in Figure 7.6 together with the corresponding along-fjord current profile, positive current is directed out of fjord. The maximum current speed is observed at the surface in both years,

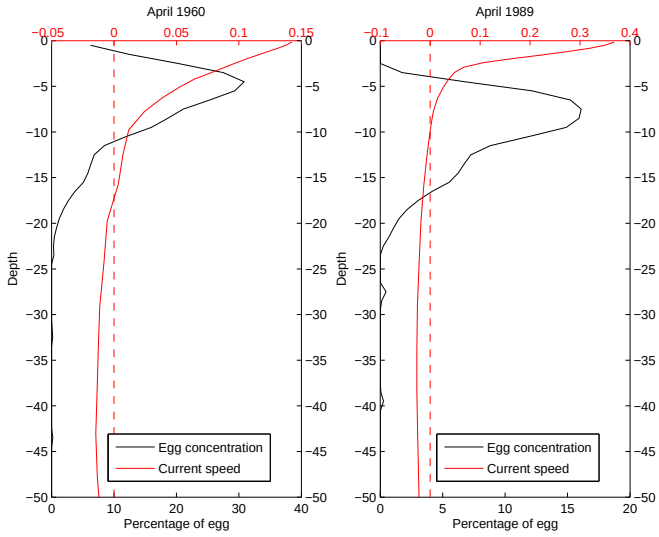

Figure 7.6: The vertical distribution of eggs together with the local along-fjord current speed from April 1960 (left) and 1989 (right), at a station in Sørfolda (Figure 2.2), positive direction is out of the fjord.

but with different scales. In 1960 the outflowing surface current is close to 0.15 m/s, and approximately 0.36 m/s in 1989. The depth of the surface layer is largest in 1960, this was also observed in the salinity profile. This results in a greater portion of eggs being situated within the outgoing surface

layer in 1960, than in 1989. In 1989 only a small percentage of eggs are at a depth with outflowing water, the rest of the eggs are in a location with no currents or inward currents. This explains the results showing larger degree of retention towards the end of April 1989 compared to 1960.

7.3 Separation and mixing of ANC and CC eggs

When discussing the separation and mixing between Arcto-Norwegian Cod (ANC) and Norwegian Coastal Cod (CC) it is assumed that when CC eggs are transported out of the fjord, the probability of mixing between ANC and CC is high. Whenever the CC eggs are retained within the fjord system the two populations are separated.

After approximately 21 days the eggs hatch into larvae. Almost immediately the larvae are able to move vertically in relation to prey density. Data from Lofoten indicate that the highest concentration of cod larvae is between 10-30 m depth (Ellertsen *et al.*, 1984). The results shown in section 6.1 demonstrate that particles travelling below 10 m depth have a small horizontal spreading. If the eggs are retained inside the fjord system at the time of hatching, it is likely that the retention will continue also during the larval stage.

7.3.1 Importance of buoyancy

The neutral buoyancy of CC eggs is the only variable used in these simulations to evaluate the separation between ANC and CC. However, the results show that buoyancy of eggs are an important factor deciding the spreading of the eggs. The first approach with transport of eggs at 1 m depth, shows what would happen to pelagic eggs in this fjord system. Especially during 1989 a large portion of pelagic eggs was spreading out on a large area. When the buoyancy distribution of CC eggs were included in the simulations, the amount of eggs being retained within the fjord increased. This means that the potential for being advected out of the fjord is highly present. However, since the mesopelagic CC eggs are heavier than the surface layer, they avoid mixing with ANC outside the fjord. There is also a variability in the transport within the buoyancy distribution of CC eggs. The lightest buoyancy group has the highest probability (6.9%) of being transported out of the fjord and being mixed with ANC eggs. The three heaviest buoyancy groups, containing 66% of the eggs, have minor leakage at all times and are separated from ANC eggs. Modeling studies in a fjord on the western coast

of Norway done by Asplin *et al.* (1999) also acknowledged the danger for eggs and larvae to be advected out of the fjord in the surface layer. They indicated that species have adapted the depth of spawning and the buoyancy of eggs to reduce dispersal of younger stages. The results shown here (Figure 7.5) indicate that CC have adapted their spawning behavior to increase the retention of eggs inside a fjord system.

7.3.2 Choosing spawning grounds

A significant difference between ANC and CC is the different spawning grounds. The ANC spawn in Vestfjorden, where the eggs will be lighter than the mixed layer, while the CC spawn inside the fjords where the eggs will be heavier than the mixed layer. The CC eggs will be mesopelagically distributed inside Folda, but pelagically distributed in Vestfjorden where the surface salinity is normally around 33. This is a major factor maintaining the separation between ANC and CC.

The selection of stratified water masses as spawning grounds to prevent egg stages from dispersion was discussed by Salvanes *et al.* (2004), which in turn cause the CC to develop into different coastal and fjord sub-populations adapted to the local environment.

Inside the fjord system of Folda there are spatial variations in the transport of eggs. Figure 6.7 shows that eggs spawned in Vinkfjord travel a longer distance away from their origin than all other spawning grounds. The reason for this might be the small amount of fresh water input to the fjord and close connection to the mouth. Spawning activity in Vinkfjord is likely to cause mixing between ANC and CC. These results are coherent with the information about spawning and juvenile distribution in Figure 2.4, showing that Vinkfjord is a spawning ground but not a nursery ground.

7.3.3 Seasonal and interannual variations

The results show that the retention of CC eggs within Folda varies with varying spawning time. In 1960 the spreading of eggs is highest in late spring, compared to 1989 when the spreading was highest in early spring. The main causes of this is assumed to be different onset of the estuarine circulation and change in surface salinity.

The peak spawning time for CC is towards the end of April, while the ANC reach a spawning maximum at the beginning of April. From Table 6.3 a distinct difference in transport of eggs spawned on 1^{st} and 15^{th} April is seen. For early spawners the retention is largest in 1960, causing separation between ANC and CC in 1960 but more mixing in 1989. For late spawners

the retention is strongest in 1989, resulting in mixing in 1960 and separation in 1989. This proves that the seasonal variations are on the same scale as the interannual variations. Meaning that the spawning time is important, and changes might have a large effect on the final distribution of eggs.

A clear variation between 1960 and 1989 is seen as well. The main difference is seen in the fresh water input, being about twice as large in 1989. The fresh water discharge causes changes in the estuarine circulation and in the salinity of the brackish layer as noted earlier. The transport of eggs at fixed depths shows a significant difference between the years, being a reflection of the currents at constant depths. During the whole spawning period the total amount of eggs leaving the fjord is 2.7% in both 1960 and 1989 included all buoyancy groups and all spawning times. Hence the total amount of mixing between ANC and CC eggs do not change between the years, but the time of mixing is different. In March and beginning of April the separation is stronger in 1960 than in 1989, contrary to the end of April and May where the separation is more pronounced in 1989 than in 1960. The favorable time for spawning to achieve separation is changing between the years. However, these two years show that the mixing between ANC and CC is limited and constant between years, when considering all release times. When concentrating on the two last spawning times, being the time when CC spawn, there is a significant difference between 1960 and 1989. Then the total amount of eggs leaving the fjord is 3.7% in 1960 and 0.9% in 1989. Hence the mixing between CC and ANC is largest in 1960, and 1989 shows a strong separation between the populations.

These results confirm that the two populations of cod, CC and ANC, are separated geographically during the egg stage and the mixing between them is limited. Earlier work on cod recruitment in northern Norway also acknowledged different early life history of ANC and CC (Løken *et al.*, 1994). Furthermore, they discussed juvenile segregation due to different bottom settling strategies. Knutsen *et al* (2007) sampled eggs from CC in 20 Norwegian fjords throughout a large geographical area. The results revealed a pattern with higher density of pelagic eggs inside sheltered fjord habitats along the Norwegian coast. Jorde *et al* (2007) found indications of local coastal cod populations within a geographical extent of 30 km, on the scale of local fjords. All these results confirms the existence of separated CC populations inside different fjords. This might explain the dissimilar pattern of decline in cod abundance in Skagerrak.

7.4 The impact of climate change

The climate, meaning the average weather, is not constant and varies on different time scales. A global warming is observed on top of these natural variations, caused by anthropogenic emissions of greenhouse gases. This warming is expected to continue in the future, which may have large impacts on the climate. Downscaling of climate models show a temperature increase of 1.6° in northern Norway in 50 years (Alfsen, 2001). The precipitation is expected to increase, up to a seasonal average of 7.8%. Even warmer and wetter years are probable to occur more often, being similar to 1989. Meaning that the situation observed in 1989 is likely to occur more frequently in the future.

In 1989 the mixing between ANC and CC occurred in early spring, and separation was stronger late in spring. With late April as the time of maximized spawning, this pattern favors separation. If years like 1989 occur more often and might even be warmer and wetter, these results show increased separation between ANC and CC eggs. The amount of mixing occurring early in 1989 was caused by early onset of estuarine circulation, but weaker stratification than later. Hence separation is depending on a strong stratification, which might increase due to climate change. Therefore the climate change is expected to increase the separation between ANC and CC during early life stages, caused by the retention of CC eggs.

This approach only includes physical processes maintaining the separation between ANC and CC at early life stages. Even though these results indicate strong future mechanisms to keep the CC inside the fjords, the actual survival of the offspring is not included. Salvanes *et al* (1992) found that the advection of zooplankton into a fjord might give large interannual variability in cod production. In a fjord with a sill the interaction with the coastal areas might be weak and only periodic, causing limitations on food availability. How this interaction will be affected by the climate change is not easy to predict.

Chapter 8

Summary and conclusion

A circulation model was used to simulate the estuarine circulation in a fjord in northern Norway. The model managed to reproduce the main features in the fjord system, consisting of a strong outflow in the surface layer and a weaker inflow below.

The estuarine circulation is shown to have strong seasonal variations, highly depending on the fresh water input. The onset of melting season varies between years, with following variations in volume flux of fresh water discharge.

The vertical distribution of CC eggs is found to depend on the local salinity structure. Hence the surface concentration of eggs changes with season and between years. A low-saline surface layer results in a mesopelagic distribution, with most eggs situated below the surface layer. Small variations in buoyancy cause vertical displacements. The vertical position controls the transport of eggs, strongly affected by the strong surface flow.

Seasonal variability is shown to be on the same scale as interannual variability. Considering the last part of the spawning period a stronger separation between ANC and CC is observed in 1989 compared to 1960. Future climate change might cause stronger separation between ANC and CC eggs. These results show that most CC eggs stay very close to their origin. Supporting that there are several local populations of CC along the coast, with limited amount of exchange between the populations. Strong physical mechanisms support the maintenance of local cod populations.

Since the CC is highly self-recruiting, this is a major challenge for managing the stocks. Overfishing in a fjord might cause the stock to suffer major damage and it will have difficulties to recover. While at the same time stocks in the neighboring fjord might be sustainable and suffer no depletion. Weak interaction between local populations demands local administration of the fish quotas.

Future work

These results show a need for better wind resolution in the model run. This can be done by downscaling the wind field using a model setup for this specific domain.

For better model results the model domain should contain Vestfjorden to include the effects of upwelling and downwelling during major wind events. Also the maximum depth should be increased. In this way the fjord system will be more realistic and may even host renewal events.

Only two years are used in this study. To study these processes further several different years should be included to elaborate on the different mechanisms causing separation within years and between years.

More information about the spawning period of the CC is needed. Kjesbu (1988) indicated that CC spawns later than ANC, the results presented here show that the mixing between CC and ANC are subjected to substantial seasonal variations.

Appendix A

Data from Folda

On 4^{th} and 5^{th} April 2007 Johan Hjort collected hydrographical data in Folda. Totally 10 CTD-stations were taken inside the fjord system. Figure A.1 shows the locations of the stations, together with the salinity profile using the same color.

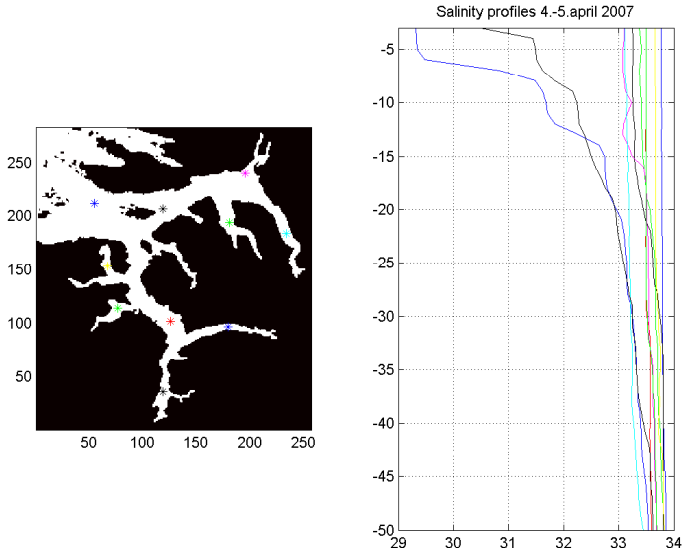

Figure A.1: Salinity profiles in Folda in the upper 50 m, colors correspond to each other.

The two stations with lowest surface salinity is located at the inner part of Sørfolda (∼29.3) and Leirfjorden (∼30.5). These two stations show a strong stratification and a surface layer only about 5-10 m deep. All other stations have a surface salinity between 33 and 33.8, and with very small variations

in the upper 50 m.

In Figure A.2 the exact same data are plotted, but now showing the upper 200 m and with a smaller range of salinities neglecting the freshest stations. Some variability is seen in the upper part, with salinities ranging from 33 to 33.8. The stations with lowest surface salinity is located in Nordfolda. Below about 60 m the differences between stations are reduced, and further decreasing downwards. In the upper 100 m the vertical variations are quite small, but between 100 m and 180 m is a deep halocline.

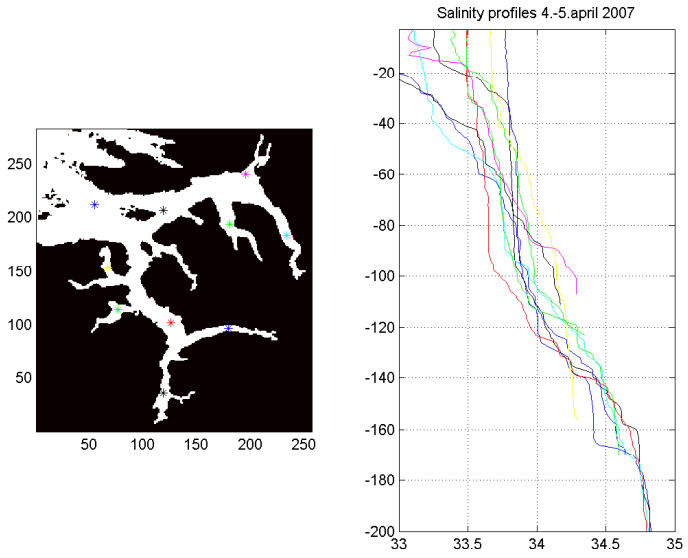

Figure A.2: Salinity profiles in Folda in the upper 200 m, with shorter range in salinity neglecting the freshest stations.

The weather conditions at the time of these observations should be added in these considerations. The reason is the strong winds on 4^{th} and 5^{th} April 2007. Outside Folda the wind strength was around 19.8 m/s and with a dominantly westerly component. This means that strong winds where directed straight into the fjord at the time of the measurements. The exact impact of these weather conditions are not easy to quantify, but strong mixing would be expected. The winds could be so strong that the normal estuarine circulation may be reversed with inflow in the upper layer and outflow below. The surface salinity observed could then be higher than what would normally be the case.

On this cruise also eggs where collected at the CTD-stations. The number of eggs collected at the inner part of Sørfolda are shown in Figure A.3, together with the salinity profile at the station. Totally 67 eggs where sam-

pled at this station. From the surface and down to 15 m depth 32 eggs where collected, a percentage of 48. In the layer at 15-30 m 30% of the eggs where found, at 30-45 m depth 19% and between 45 m and 60 m 3% of the eggs. The eggs show a pelagic distribution.

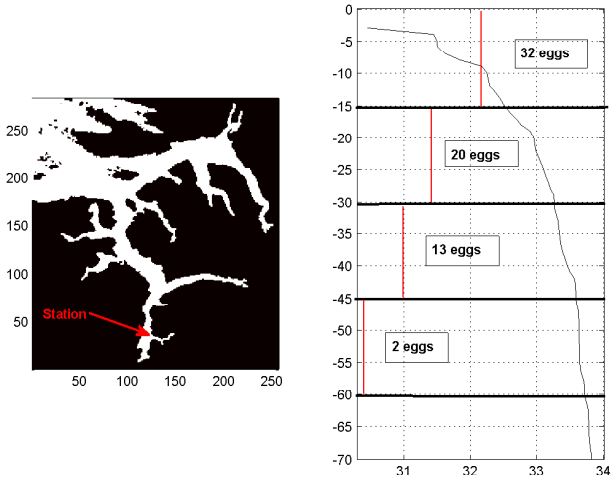

Figure A.3: Salinity profile and corresponding egg distribution collected.

References

Alfsen, K.H. 2001. *Klimaet er i endring.* Cicero. 12.

Árnason, E., & Pálsson, S. 1996. Mitochondrial cytochrome b DNA sequence variation of Atlantic cod (*Gadus morhua* L.) from Norway. *Molecular Ecology*, **5**, 715–724.

Asplin, L., Salvanes, A.G.V., & Kristoffersen, J.B. 1999. Nonlocal wind-driven fjord-coast advection and its potential effect on plankton and fish recruitment. *Fisheries oceanography*, **8**(4), 255–263.

Asplin, L., Boxaspen, K., & Sandvik, A.D. 2002. Lakselus - en trussel for villaksen, Miljørapporten 2002. *Fisken og havet*, **særnr.2**, 144–149.

Aure, J., & Pettersen, R. 2004. Miljøundersøkelser i norske fjorder 1975-2000. *Fisken og Havet*, **8**, 176.

Bergstad, O.A., Jørgensen, T., & Dragesund, O. 1987. Life history and ecology of the gadoid resources of the Barents Sea. *Fisheries Research*, **5**, 119–161.

Chapman, D.C. 1985. Numerical treatment of cross-shelf open boundaries in a barotropic coastal ocean model. *Journal of Physical Oceanography*, **15**, 1060–1075.

Dyer, K.R. 1997. *Estuaries - A Physical Introduction.* 2nd edn. Wiley.

Ellertsen, B., Fossum, P., Solemdal, P., Sundby, S., & Tilseth, S. 1984. A case study on the distribution of cod larvae and availability of prey organisms in relation to physical processes in Lofoten. *Pages 453–477 of:* Dahl, E., Danielsen, D.S., Moksness, E., & Solemdal, P. (eds), *The propagation of cod (Gadus morhua L.) Flødevigen rapportserie*, vol. 1.

Ellertsen, B., Fossum, P., Solemdal, P., & Sundby, S. 1989. Relation between temperature and survival of eggs and first-feeding larvae of northeast

Arctic cod (*Gadus morhua L.*). *Rapp. P.-v. Réun. Cons. int. Explor. Mer.*, **191**, 209–219.

Engedahl, E., Ådlandsvik, B., & Martinsen, E.A. 1998. Production of monthly mean climatology archieves for the Nordic Seas. *Journal of Marine Systems*, **14**, 1–26.

Espeland, S.H., Gundersen, A.F, Olsen, E.M, Knutsen, H., Gjøsæter, J., & Stenseth, N.C. 2007. Home range and elevated egg densities within an inshore spawning ground of coastal cod. *ICES Journal of Marine Science*, **64**, 920–928. doi:10.1093/icesjms/fsm028.

Farmer, D.M., & Freeland, H.J. 1983. The physical oceanography of fjords. *Prog.Oceanog.*, **12**, 147–220.

Flather, R.A. 1976. A tidal model of the northwest European continental shelf. *Memories de la Societe Royale des Sciences de Liege*, **10**, 141–164.

Furnes, G.K., & Sundby, S. 1981. Upwelling and wind induced circulation in Vestfjorden. *Pages 152–178 of:* Sætre, R., & Mork, M. (eds), *Proceedings from Norwegian Coastal Current Symposium, Geilo, 9-12 September 1980*, vol. 1.

Haidvogel, D.B., Arango, H., Budgell, W.P., Cornuelle, B.D., Curchitser, E., Di Lorenzo, E., Fennel, K., Geyer, W.R., Hermann, A.J., Lanerolle, L., Levin, J. McWilliams, J.C., Miller, A.J., Moore, A.M., Powell, T.M., Shchepetkin, A.F., Sherwood, C.R., Signell, R.P., Warner, J.C., & Wilkin, J. 2007. Ocean forecasting in terrain-following coordinates: Formulation and skill assessment of the Regional Ocean Modeling System. *J. Comput. Phys.*, 1–30. doi:10.1016/j.jcp.2007.06.016.

Hjort, J. 1914. Fluctuation in the great fisheries of northern Europe viewed in the light of biological research. *Rapp. P.-v Réun. Cons. int. Explor. Mer*, **20**, 1–228.

Jakobsen, T. 1987. Coastal cod in northern Norway. *Fisheries Research*, **5**, 223–234.

Jorde, P.E., Knutsen, H., Espeland, S.H., & Stenseth, N.C. 2007. Spatial scale of genetic structuring in coastal cod *Gadus morhua* and geographic extent of local populations. *Mar. Ecol. Prog. Ser.*, **343**, 229–237. doi:10.3354/meos06922.

Kjesbu, O.S. 1988. Fecundity and maturity of cod. *ICES Council Meeting*, **1988/G:28**, 16.

Kjesbu, O.S., Kryvi, H., Sundby, S., & Solemdal, P. 1992. Buoyancy variations in eggs of Atlantic cod in relation to chorion thickness and egg size: theory and observations. *Journal of Fish Biology*, **41**, 581–599.

Knutsen, H., Olsen, E.M., Cianneli, L., Espeland, S.H., Knutsen, J.A., Simonsen, J.H., Skreslet, S., & Stenseth, N.C. 2007. Egg distribution, bottom topography and small-scale cod population structure in a coastal marine system. *Mar. Ecol. Prog. Ser.*, **333**, 249–255.

Løken, S., Pedersen, T., & Berg, E. 1994. Vertebrae number as an indicator for the recruitment mechanism of coastal cod of northern Norway. *ICES Marine Science Symposia*, **198**, 510–519.

Martinsen, E.A., & Engedahl, H. 1987. Implementation and testing of a lateral boundary scheme as an open boundary condition in a barotropic ocean model. *Coastal Engineering*, **11**, 603–627.

Moe, H., Ommundsen, A., & Gjevik, B. 2002. A high resolution tidal model for the area around The Lofoten Islands, northern Norway. *Continental shelf research*, **22**, 485–504.

Mohus, Å., & Haakstad, M. 1984. *Straumbukta i Sørfold, en kortfattet hydrografisk og hydrokjemisk kartlegging.* Nordland distriktshøgskole, Mat/Nat fagseksjon. 55.

Mork, J., & Giæver, M. 1999. Genetic structure of cod along the coast of Norway: Results from isozyme studies. *Sarsia*, **84**(2), 157–168.

NVE. 2002. *Avrenningskart for Norge, 1961-1990.* The Norwegian Water Resources and Energy Directorate, Hydrological department.

Ottersen, G., Planque, B., Belgrano, A., Post, E., Reid, P.C, & Stenseth, N.C. 2001. Ecological effects of the North Atlantic Oscillation. *Oecologia*, **128**, 1–14.

Pogson, G.H., & Fevolden, S.E. 2003. Natural selection and the genetic differentiation of coastal and Arctic populations of the Atlantic cod in northern Norway: a test involving nucleotide sequence variation at the pantophysin (PanI) locus. *Molecular Ecology*, **12**, 63–74.

Reffhaug, P. 2006. *Kystbok for Sørfold - om Sørfolda og Nordfolda.* Sørfold kommune.

Rinde, E., Bjørge, A., Eggereide, A., & Tuftland, G. (eds). 1998. *Kystøkologi - den ressursrike norskekysten.* Universitetsforlaget. Pages 103–131.

Rollefsen, G. 1933. The otoliths of the cod: preliminary report. *Fiskeridirektoratets skrifter, Serie Havundersøkelser*, **4**(3), 14.

Salvanes, A.G.V., Aksnes, D.L., & Giske, J. 1992. Ecosystem model for evaluating potetial cod production in a west Norwegian fjord. *Mar. Ecol. Prog. Ser.*, **90**, 9–22.

Salvanes, A.G.V., Skjæraasen, J.E., & Nilsen, T. 2004. Sub-populations of coastal cod with different behavior and life-history strategies. *Mar. Ecol. Prog. Ser.*, **267**, 241–251.

Shchepetkin, A.F., & McWilliams, J.C. 2005. The regional oceanic modeling system (ROMS): a split-explicit, free-surface, topography-following-coordinate oceanic model. *Ocean Modeling*, **9**, 347–404.

Sælen, O.H. 1967. Some features of the hydrography of Norwegian fjords. *Pages 63–70 of:* Lauff, G.H. (ed), *Estuaries.* Washington D.C.: AAAC.

Solemdal, P., & Sundby, S. 1981. Vertical distribution of pelagic fish eggs in relation to species, spawning behavior and wind conditions. *ICES Council Meeting*, **1981/G:77**, 27.

Statens Kartverk, Sjøkartverket. 1998. *Den Norske Los.* 5th edn. Farvannsbeskrivelse, Rørvik - Lødingen og Andenes. Pages 168–172.

Stenevik, E.K., Sundby, S., & Agnalt, A.L. 2008. Buoyancy of eggs of Norwegian coastal cod from different areas along the coast. *ICES Journal of Marine Science.* (accepted).

Stigebrandt, S. 1981. A mechanism governing the estuarine circulation in deep, strongly stratified fjords. *Estuarine, Coastal and Shelf Sciences*, **13**, 197–211.

Sundby, S. 1980. Utvikling innen oseanografisk forskning i Vestfjorden. *Fisken Hav.*, **1**, 11–25.

Sundby, S. 1982. Vestfjordundersøkelser 1978 - Fresh water budget and wind conditions. *Fisken Hav.*, **1**, 1–30.

Sundby, S. 1983. A one-dimensional model for the vertical distribution of pelagic fish eggs in the mixed layer. *Deep-Sea Research*, **30**, 645–661.

Sundby, S. 1991. Factors affecting the vertical distribution of eggs. *ICES Marine Science Symposia*, **192**, 33–38.

Sundby, S., & Bratland, P. 1987. Kartlegging av gytefeltene for Norsk-Arktisk torsk i Nord-Norge og beregning av eggproduksjon i årene 1983-1985. *Fisken Hav.*, **1**, 1–58.

Sundby, S., & Godø, O.R. 1994. Life history of arcto-Norwegian cod stock. *ICES Coop. Res. Rep.*, **205**, 12–45.

Svendsen, H., & Thompson, R.O.R.Y. 1978. Wind-driven circulation in a fjord. *Journal of Physical Oceanography*, **8**, 703–712.

Thygesen, U.H., & Ådlandsvik, B. 2007. Simulating vertical turbulent dispersal with finite volumes and binned random walks. *Mar. Ecol. Prog. Ser.*, **347**, 145–153.

Umlauf, L., & Burchard, H. 2003. A generic length-scale equation for geophysical turbulence models. *Journal of Marine Research*, 235–265.

Vikebø, F.B., Sundby, S., & Ådlandsvik, B. 2005. Drift patterns of eggs from Coastal cod and Arcto-Norwegian cod - adaptive egg buoyancy? *Pages 115–141 of:* Vikebø, F.B, *The impact of climate on early stages of Arcto-Norwegian cod - a model approach.* Ph.D. thesis.

Ådlandsvik, B. 2000. *VertEgg - A toolbox for simulation of vertical distributions of fish eggs Version 1.0.* Institute of Marine Research. 66.

Ådlandsvik, B., & Sundby, S. 1994. Modeling the transport of cod larvae from the Lofoten area. *ICES Marine Science Symposia*, **198**, 379–392.